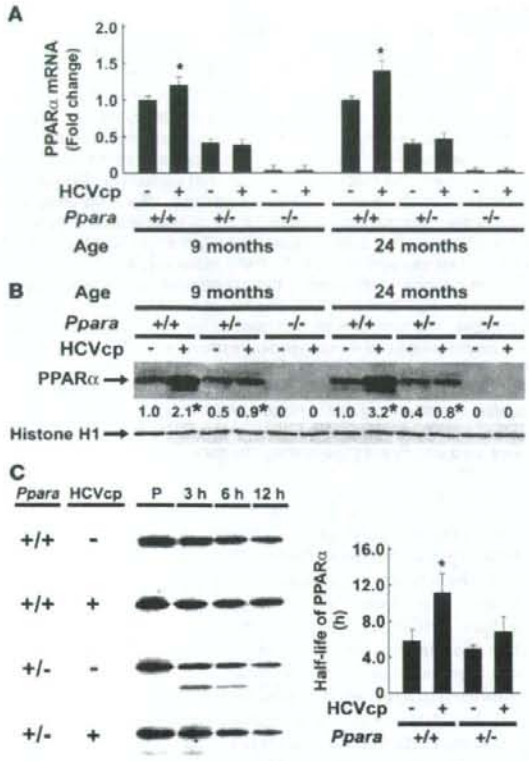


**Figure 6**
Persistent PPARα activation in *Ppara*$^{+/+}$:HCVcpTg mice. (**A**) PPARα mRNA levels. Total RNA was prepared from each mouse, and PPARα mRNA levels were determined by RT-PCR, normalized by those of GAPDH, and subsequently normalized by those of 9-month-old *Ppara*$^{+/+}$ nontransgenic mice. Results are expressed as the mean ± SD ($n$ = 6 /group). (**B**) Immunoblot analysis of nuclear PPARα. The nuclear fraction obtained from each mouse (100 μg protein) was loaded in each well. The band of histone H1 was used as the loading control. Results are representative of 6 independent experiments. The band intensity was quantified densitometrically, normalized by that of histone H1, and subsequently normalized by that in 9-month-old *Ppara*$^{+/+}$ nontransgenic mice. The mean value is expressed under each band. *$P$ < 0.05 compared with nontransgenic mice of the same age and *Ppara* genotype. (**C**) Pulse-chase experiments for 3, 6, and 12 h and pulse-label (P) experiments for nuclear PPARα using isolated mouse hepatocytes. Left: labeled PPARα bands on x-ray film. Pulse-label and pulse-chase experiments were performed as described in Methods. Results are representative of 4 independent experiments. Right: half-life of PPARα. The band intensity was measured densitometrically and subsequently normalized by that of the pulse-label experiments. The percentage of the band intensity was plotted, and the half-life of PPARα was calculated. Results obtained from 4 independent experiments are expressed as the mean ± SD. *$P$ < 0.05 compared with nontransgenic mice in the same *Ppara* genotype.

PPARα influences the stability of RXRα (28), it is plausible that the core protein would affect its action in nuclei through an interaction with the PPARα-RXRα heterodimer and stabilization of PPARα.

*Development of hepatic steatosis and HCC with long-term clofibrate treatment in Ppara*$^{+/-}$*:HCVcpTg mice.* To further confirm the significance of persistent PPARα activation on core protein–induced pathological changes, *Ppara*$^{+/-}$ and *Ppara*$^{+/-}$:HCVcpTg mice were fed a standard diet containing 0.05% clofibrate for 24 months. Interestingly, hepatic steatosis appeared in the clofibrate-treated *Ppara*$^{+/-}$:HCVcpTg mice, but not in the *Ppara*$^{+/-}$ mice under the same treatment conditions (Figure 7, A and B). Similar to our observations in *Ppara*$^{+/+}$:HCVcpTg mice not treated with clofibrate, aberrant mitochondria with discontinuous outer membranes and decreased palmitic acid β-oxidation activity were found only in the clofibrate-treated *Ppara*$^{+/-}$:HCVcpTg mice (Figure 7, A and C). In addition, levels of MCAD mRNA; AOX, and CYP4A1 proteins; PPARα mRNA; and nuclear PPARα protein were higher in the clofibrate-treated *Ppara*$^{+/-}$:HCVcpTg mice than in the clofibrate-treated *Ppara*$^{+/-}$ mice (Figure 7, D–F), which suggests that the degree of PPARα activation in the former group was greater than that in the latter group and similar to that in *Ppara*$^{+/+}$:HCVcpTg mice not treated with clofibrate. Finally, the incidence of HCC after clofibrate treatment was higher in *Ppara*$^{+/-}$:HCVcpTg mice (25%; 5 in 20 mice) than in *Ppara*$^{+/-}$ mice (5%; 1 in 20 mice). Therefore, these results corroborate the importance of constant PPARα activation to the pathogenesis of hepatic steatosis and HCC in the transgenic mice.

## Discussion

A novel and striking finding in this study is the absolute requirement of persistent PPARα activation for the development of HCV core protein–induced steatosis and HCC. Our data also show that the HCV core protein alone cannot induce steatosis and HCC in transgenic mice.

Mechanisms of development of steatosis in HCVcpTg mice were previously explained as an enhancement of de novo synthesis of fatty acids (29) and a decrease in MTP expression, the latter of which results in insufficient VLDL secretion from hepatocytes (30). In the present study, we revealed 2 novel mechanisms of steatogenesis in the transgenic mice, i.e., an impairment of mitochondrial β-oxidation due to the breakdown of mitochondrial outer membranes and an increase in fatty acid uptake into hepatocytes, associated with PPARα activation. PPARα activation, mitochondrial dysfunction, and hepatic steatosis appeared in 9-month-old *Ppara*$^{+/+}$:HCVcpTg mice and continued until 24 months of age, clearly preceding development of HCC. These findings thereby indicate a correlation between PPARα activation, hepatic steatosis, and HCC.

We obtained the novel and rather paradoxical finding that significant PPARα activation, which generally is expected to reduce hepatic triglyceride levels, is essential for the development of severe steatosis induced by HCV core protein. According to the results of this study, the following hypothesis concerning the development of steatosis in *Ppara*$^{+/+}$:HCVcpTg mice is proposed. First, the HCV core protein localizes partly in mitochondria (9). A recent study

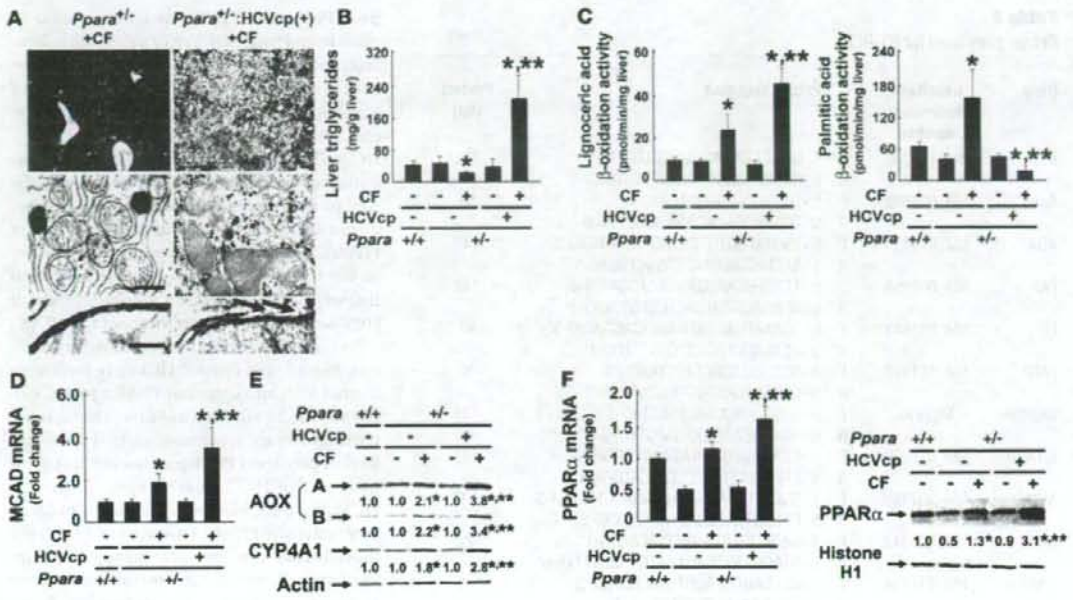


**Figure 7**

Development of hepatic steatosis by long-term treatment of clofibrate in *Ppara*$^{+/-}$:HCVcpTg mice. (**A**) Histological examination of *Ppara*$^{+/-}$ and *Ppara*$^{+/-}$:HCVcpTg mice treated with diet containing 0.05% (w/w) clofibrate for 24 months (CF). Top: Histological appearance of H&E-stained liver sections. Magnification, ×40. Microvesicular and macrovesicular steatosis were detected only in clofibrate-treated *Ppara*$^{+/-}$:HCVcpTg mice. Middle and bottom: Electron microscopic features of hepatic mitochondria. Some C-shaped mitochondria showing discontinuance of outer membranes (arrows) were found in clofibrate-treated *Ppara*$^{+/-}$:HCVcpTg mice. Scale bars: 400 nm (middle), 30 nm (bottom). (**B** and **C**) Content of liver triglycerides and lignoceric and palmitic acid β-oxidation activities. (**D**) MCAD mRNA levels. mRNA levels were normalized to those of GAPDH and subsequently normalized to those in *Ppara*$^{+/+}$ nontransgenic mice. (**E**) Immunoblot analysis of AOX and CYP4A1. Whole-liver lysate (20 μg protein) was loaded in each lane. Actin was used as a loading control. Results are representative of 6 independent experiments. (**F**) PPARα mRNA levels and nuclear PPARα contents. Left: PPARα mRNA levels. The same samples used in **D** were adopted. Right: Immunoblot analysis of nuclear PPARα. Nuclear fraction obtained from each mouse (100 μg protein) was loaded in each well. Histone H1 was used as a loading control. In **E** and **F**, the mean value of the fold changes is shown under each band. Results are representative of 6 independent experiments. Band intensity was quantified densitometrically, normalized to that of the loading control, and subsequently normalized to that in *Ppara*$^{+/+}$ nontransgenic mice. $^{*}P < 0.05$ compared with untreated mice of the same genotype; $^{**}P < 0.05$ compared with clofibrate-treated *Ppara*$^{+/-}$ mice without core protein gene. Results are expressed as mean ± SD ($n$ = 6/group).

showed that, in isolated mitochondria, the core protein directly increased $Ca^{2+}$ influx, inhibited electron transport complex I activity, and induced ROS production (31), all of which can increase the fragility of mitochondria and depress mitochondrial function. In addition, the HCV core protein also localizes in nuclei (9) and can coexist in PPARα-RXRα heterodimer through a direct interaction with the DNA-binding domain of RXRα, which enhances the transcriptional activity of PPARα target genes, such as AOX, despite the absence of PPARα ligands in cultured cells (27). The HCV core protein can also be involved in the PPARα-RXRα complex through a direct interaction with cyclic-AMP responsive element binding protein-binding protein (32), which is able to bind to PPARα (33). Thus, the core protein probably serves as a coactivator and stabilizer of PPARα in vivo, which was further confirmed in this study. Moreover, because it is also known that the core protein itself activates ERK1/2 and p38 mitogen-activated protein kinase (34), these activations might phosphorylate PPARα and thereby transactivate it (35). The core protein-induced PPARα activation enhances the basal expression of AOX and CYP4A1, which leads to increased production of ROS and dicarboxylic acids. These toxic compounds can damage mitochondrial outer membranes, which impairs the mitochondrial β-oxidation system. These damages directly induce the accumulation of long-chain fatty acids in hepatocytes. Furthermore, PPARα activation increases the expression of FAT and FATP, which promotes the influx of fatty acids from blood. Long-chain fatty acids and their CoA esters accumulated in hepatocytes are likely to act as potent detergents, which further damages the outer membranes of mitochondria. Fatty acids and their derivatives function as natural ligands of PPARα, which results in the activation of PPARα and the induction of FAT, FATP, AOX, and CYP4A1, which further accelerates mitochondrial damage, the reduction of mitochondrial β-oxidation activity, and the accumulation of fatty acids in a vicious cycle.

Persistent PPARα activation increases oxidative DNA damage because of a disproportionate increase in ROS-generating enzymes relative to the levels of degrading enzymes such as catalase and SOD, which can predispose hepatocytes to malignant transformation. In addition, persistent PPARα activation leads to increased

**Table 2**
Primer pairs used for RT-PCR

| Gene | GeneBank accession number | | Primer sequence | Product (bp) |
|---|---|---|---|---|
| ACC | NM_133360 | F | 5′-GGGCACAGACCGTGGTAGTT-3′ | 105 |
| | | R | 5′-CAGGATCAGCTGGGATACTGAGT-3′ | |
| ApoB | NM_009693 | F | 5′-TCACCCCCGGGATCAAG-3′ | 85 |
| | | R | 5′-TCCAAGGACACAGAGGGCTTT-3′ | |
| AOX | NM_015729 | F | 5′-TGGTATGGTGTCGTACTTGAATGAC-3′ | 145 |
| | | R | 5′-AATTTCTACCAATCTGGCTGCAC-3′ | |
| FAS | NM_007988 | F | 5′-ATCCTGGAACGAGAACACGATCT-3′ | 140 |
| | | R | 5′-AGAGACGTGTCACTCCTGGACTT-3′ | |
| FAT | NM_007643 | F | 5′-CCAAATGAAGATGAGCATAGGACAT-3′ | 87 |
| | | R | 5′-GTTGACCTGCAGTCGTTTTGC-3′ | |
| FATP | NM_011977 | F | 5′-ACCACCGGGCTTCCTAAGG-3′ | 80 |
| | | R | 5′-CTGTAGGAATGGTGGCCAAAG-3′ | |
| GAPDH | M32599 | F | 5′-TGCACCACCAACTGCTTAG-3′ | 177 |
| | | R | 5′-GGATGCAGGGATGATGTTCTG-3′ | |
| L-FABP | NM_017399 | F | 5′-GCAGAGCCAGGAGAACTTTGAG-3′ | 121 |
| | | R | 5′-TTTGATTTTCTTCCCTTCATGCA-3′ | |
| MCAD | NM_007382 | F | 5′-TGCTTTTGATAGAACCAGACCTACAGT-3′ | 128 |
| | | R | 5′-CTTGGTGCTCCACTAGCAGCTT-3′ | |
| MTP | NM_008642 | F | 5′-GAGCGGTCTGGATTTACAACG-3′ | 72 |
| | | R | 5′-GTAGGTAGTGACAGATGTGGCTTTTG-3′ | |
| PPARα | NM_011144 | F | 5′-CCTCAGGGTACCACTACGGAGT-3′ | 69 |
| | | R | 5′-GCCGAATAGTTCGCCGAA-3′ | |

F, forward sequence; R, reverse sequence.

cell division, as revealed by the expression of cell cycle regulators such as cyclin D1 and CDK4. Furthermore, there is little change in apoptosis, which, under normal circumstances, would remove damaged cells capable of undergoing transformation. Thus, under these conditions, it is plausible that some aberrant hepatocytes do not undergo apoptosis and develop into HCC.

It is well known that chronic activation of PPARα is associated with hepatocarcinogenesis in mice exposed to peroxisome proliferators or in mice lacking AOX expression. The common clinicopathological characteristics of HCC in these mice are multicentric HCC (20, 22, 36, 37), the well-differentiated appearance of HCC including trabecular features and often a "nodule-in-nodule" pattern (22, 36, 37), and no evidence of fibrosis or cirrhosis in the nonneoplastic liver parenchyma (22, 36), similar to that observed in *Ppara*$^{+/+}$:HCVcpTg mice. However, mice chronically exposed to peroxisome proliferators are clearly distinct from *Ppara*$^{+/+}$:HCVcpTg mice in that they have normal mitochondrial organization, increased mitochondrial β-oxidation activity, and no steatosis (16, 36). AOX-null mice are also different from *Ppara*$^{+/+}$:HCVcpTg mice with respect to mitochondrial structure (22). These detailed comparisons between the 3 mouse models reveal the importance of mitochondrial abnormalities in the pathogenesis of HCV-related diseases.

PPARα is known to regulate the hepatic expression of many proteins associated with fatty acid and triglyceride metabolism, cell division and apoptosis, oxidative stress generation and degradation, and so forth (15, 16, 20, 21, 24–26); therefore, complete deletion of the PPARα gene from mice might cause hitherto unknown influences on the pathways involved in the development of hepatic steatosis and HCC. To consider these unknown effects, *Ppara*$^{-/-}$:HCVcpTg mice were adopted in the current study. Surprisingly, almost all results from *Ppara*$^{+/-}$:HCVcpTg mice were similar to those from *Ppara*$^{-/-}$:HCVcpTg mice, which demonstrates that the presence of functional PPARα itself is not a prerequisite for the occurrence of steatosis and HCC induced by the HCV core protein. Moreover, a comparison between *Ppara*$^{+/-}$:HCVcpTg and *Ppara*$^{+/+}$:HCVcpTg mice uncovered an unexpected and important fact that the core protein–dependent pathological changes do not appear without significant activation of PPARα. Thus, it is not the presence of PPARα per se, but rather a high level of PPARα activation that seems to be essential for the development of HCV core protein–induced steatosis and HCC.

To reinforce the abovementioned hypothesis, *Ppara*$^{+/-}$ and *Ppara*$^{-/-}$:HCVcpTg mice were treated with an exogenous PPAR agonist, clofibrate, for 24 months. In *Ppara*$^{+/-}$ mice, long-term clofibrate treatment caused a certain level of persistent PPARα activation and a low incidence of HCC. Interestingly, in *Ppara*$^{+/-}$:HCVcpTg mice, clofibrate treatment induced more intensive PPARα activation and HCC at a much higher incidence, accompanied by damaged mitochondrial outer membranes, severe steatosis, and decreased mitochondrial β-oxidation activity. The results from the clofibrate-treated *Ppara*$^{+/-}$:HCVcpTg mice were similar to those of the *Ppara*$^{+/+}$:HCVcpTg mice not treated with clofibrate. Therefore, these findings further support the concept that a long-term and high level of PPARα activation is necessary for steatogenesis and hepatocarcinogenesis in HCVcpTg mice and emphasize the significant role of the HCV core protein as a PPARα coactivator in vivo.

A pulse-chase experiment showed that PPARα was stabilized in hepatocyte nuclei in mice expressing the HCV core protein. Many nuclear receptors, including PPARα and RXRα, are known to be degraded by the ubiquitin-proteasome system (38), which plays an important role in modulating the activity of nuclear receptors. Further studies will be needed to clarify whether the core protein influences the ubiquitin-proteasome pathway.

Recent studies have shown conflicting result, i.e., that PPARα was downregulated in the livers of chronic hepatitis C patients (39, 40). Although the association between PPARα function and chronic HCV infection remains a matter of controversy in humans, the changes observed in the transgenic mice resemble in many ways the clinicopathological features of chronically HCV-infected patients; both show a high frequency of accompanying steatosis (10, 40, 41), increased accumulation of carbon 18 monounsaturated fatty acids in the liver (42), mitochondrial dysfunction (43), increased insulin resistance (44) and oxidative stress (45, 46), male-preferential (2) and multicentric occurrence of HCC (47, 48), and the well-differentiated appearance of HCC, including trabecular features and often a "nodule-in-nodule" pattern (47, 48). Thus, it is postulated that the mechanism of steatogenesis and hepatocarcinogenesis we proposed may partially apply to patients with chronic HCV infection. If so, therapeutic interventions to alleviate persistent and excessive PPARα activation might be beneficial in the prevention of HCC. To clarify the exact relationship between PPARα activation and HCV-induced hepatocarcinogenesis in humans, further

experiments using noncancerous liver tissues obtained from HCV-related HCC patients and using mice carrying human PPARα and HCV core protein genes are needed.

In conclusion, we clarified for the first time that persistent and potent PPARα activation is absolutely required for the development of severe steatosis and HCC induced by HCV core protein. In addition, we uncovered paradoxical and specific functions of PPARα in the mechanism of steatogenesis mediated by the core protein. Our results offer clues in the search for novel therapeutic and nutritional management options, especially with respect to neutral lipids, for chronically HCV-infected patients.

## Methods

*Mice.* The generation of HCVcpTg mice and *Ppara*$^{-/-}$ mice was described previously (7, 24, 49). Male HCVcpTg mice and female *Ppara*$^{-/-}$ mice were mated, and F1 mice bearing the HCV core protein gene were intercrossed to produce F2 mice. *Ppara*$^{+/+}$, *Ppara*$^{+/-}$, and *Ppara*$^{-/-}$ mice bearing the HCV core protein gene, designated as *Ppara*$^{+/+}$:HCVcpTg, *Ppara*$^{+/-}$:HCVcpTg, and *Ppara*$^{-/-}$:HCVcpTg mice, in the F4 generation were subjected to serial analyses. Because HCC develops preferentially in male HCVcpTg mice (9), male mice were analyzed. Age-matched male *Ppara*$^{+/+}$ mice without the core protein gene were used as controls. For identifying genotypes, genomic DNA was isolated from mouse tails and amplified by PCR. Primer pairs were designed as described elsewhere: 5′-GCCCACAGGACGTTAAGTTC-3′ and 5′-TAGTTCACGCCGTCCTCCAG-3′ for the HCV core gene (7) and 5′-CAGAGCAACCATCCAGATGA-3′ and 5′-AAACGCAACGTAGAGTGCTG-3′ for the PPARα gene (24). Amplified alleles for HCV core and PPARα genes were 460 and 472 base pairs, respectively. Five mice per cage were fed a routine diet and were kept free of specific pathogens according to institutional guidelines. For the clofibrate treatment experiments, 2-month-old male *Ppara*$^{+/+}$ and *Ppara*$^{-/-}$:HCVcpTg mice were randomly divided into 2 groups ($n$ = 20 in each group) and were fed either a routine diet or one containing 0.05% (w/w) clofibrate (Wako Pure Chemicals Industries) for 24 months. All mice were killed by cervical dislocation before their livers were excised. If a hepatic tumor was present, the tumor was removed and subjected to histological analysis, and the remaining liver tissues were used for biochemical analyses. All animal experiments were conducted in accordance with animal study protocols outlined in the *Guide for the Care and Use of Laboratory Animals* prepared by the National Academy of Sciences and approved by the Shinshu University School of Medicine.

*Preparation of nuclear, mitochondrial, and cytosolic fractions.* Approximately 400 mg of liver tissue was minced on ice and transferred to 10% (w/v) isolation buffer (250 mM sucrose in 10 mM Tris-HCl [pH 7.4] and 0.5 mM EGTA and 0.1% bovine serum albumin [pH 7.4]). The samples were gently homogenized by 10–20 strokes with a chilled Dounce homogenizer (Wheaton) and loose-fitting pestle. The homogenate was centrifuged at 500 × *g* for 5 min at 4°C. The supernatant was retained, and the resulting pellet was resuspended with isolation buffer and centrifuged at 4,500 *g* for 10 min at 4°C. The pellet fraction was suspended again and centrifuged at 20,000 × *g* for 1 h at 4°C, and the resulting pellet was used as the nuclear fraction. The combined supernatant fractions were centrifuged at 7,800 × *g* for 10 min at 4°C to obtain a crude mitochondria pellet. This pellet was resuspended with isolation buffer, centrifuged at 7,800 × *g* for 10 min at 4°C, and used as the mitochondrial fraction. Finally, all supernatant fractions were collected and centrifuged at 20,000 × *g* for 30 min at 4°C, and the resulting supernatant was used as the cytosolic fraction.

*Immunoblot analysis.* Protein concentrations were measured colorimetrically with a BCA Protein Assay kit (Pierce). For the analysis of fatty acid–metabolizing enzymes, hepatocyte mitochondrial fractions or whole-liver lysates (20 μg protein) were subjected to 10% SDS-PAGE (16). For analysis of PPARα, nuclear fractions (100 μg protein) were used. For analysis of other proteins, whole lysates or cytosolic fractions (50 μg protein) were subjected to electrophoresis. After electrophoresis, the proteins were transferred to nitrocellulose membranes, which were incubated with the primary antibody and then with alkaline phosphatase-conjugated goat anti-rabbit or anti-mouse IgG. Antibodies against HCV core protein, fatty acid–metabolizing enzymes, CYP4A1, catalase, and PPARα were described previously (9, 16, 24, 50). Antibodies against other proteins were purchased commercially: cytochrome *c* antibody from BD Transduction Laboratories and other antibodies from Santa Cruz Biotechnology. The band of actin or histone H1 was used as the loading control. The band intensity was measured densitometrically, normalized to that of actin or histone H1, and subsequently expressed as fold changes relative to that of *Ppara*$^{+/+}$ nontransgenic mice.

*Analysis of mRNA.* Total liver RNA was extracted using an RNeasy Mini Kit (Qiagen), and cDNA was generated by SuperScript II reverse transcriptase (Gibco BRL). Quantitative RT-PCR was performed using a SYBR green PCR kit and an ABI Prism 7700 Sequence Detection System (Applied Biosystems). The primer pairs used for RT-PCR are shown in Table 2. The mRNA level was normalized to the GAPDH mRNA level and subsequently expressed as fold changes relative to that of *Ppara*$^{+/+}$ nontransgenic mice.

*Light microscopy and immunohistochemical analysis.* Small blocks of liver tissue from each mouse were fixed in 10% formalin in phosphate-buffered saline and embedded in paraffin. Sections (4 μm thick) were stained with hematoxylin and eosin. For immunohistochemical localization of PCNA and 8-OHdG, other small blocks of liver tissue were fixed in 4% paraformaldehyde in phosphate-buffered saline. Sections (4 μm thick) then were affixed to glass slides and incubated overnight with mouse monoclonal antibodies against PCNA (1:100 dilution; Santa Cruz) or 8-OHdG (1:10 dilution; Japan Institute for the Control of Aging). Sections were immunostained using EnVision+ kit, with 3,3′-diaminobenzidine as a substrate (DAKO). Hepatocytes positive for PCNA or 8-OHdG were examined in 10 randomly selected ×400 microscopic fields per section. Two-thousand hepatocytes were examined for each mouse, and the number of immunostained hepatocyte nuclei was expressed as a percentage.

*Assessment of hepatocyte apoptosis.* TUNEL assay was performed using a MEBSTAIN Apoptosis Kit II (Medical & Biological Laboratories). Two thousand hepatocytes were examined for each mouse, and the number of TUNEL-positive hepatocytes was expressed as a percentage.

*Pulse-label and pulse-chase experiments.* Parenchymal hepatocytes were isolated by the modified *in situ* perfusion method (51). After perfusion with 0.05% collagenase solution (Wako), the isolated hepatocytes were washed 3 times by means of differential centrifugation and the dead cells were removed by density-gradient centrifugation at 500 *g* for 3 min at 4°C on Percoll (Amersham Pharmacia Biotech). The live hepatocytes were washed and suspended in William's E medium containing 5% FBS. When the viability of the isolated hepatocytes exceeded 85% as determined by the trypan blue exclusion test, the following experiments were conducted. The isolated hepatocytes were washed twice and incubated in methionine-free medium containing 5% dialyzed FBS for 1 h at 37°C. The medium was replaced with the same medium containing 300 mCi/ml of [$^{35}$S]methionine (Amersham Pharmacia Biotech). After a 3-h incubation, the labeled medium was exchanged for the standard medium, and the preparation was chased for 3, 6, or 12 h. The labeled cells were washed, homogenized, and centrifuged at 800 *g* for 5 min at 4°C to obtain a crude nucleus pellet. This pellet was resuspended with isolation buffer and centrifuged at 20,000 *g* for 1 h at 4°C to prepare the nuclear fraction. The levels of radioactivity in the homogenates of the pulse-labeled preparations were similar between the transgenic and the nontransgenic mice, which suggested that the [$^{35}$S]methionine uptake capacity in the former hepatocytes was similar to that in the latter. The nuclear fraction was lysed in RIPA buffer (10 mM Tris-HCl, pH 7.4; 0.2% sodium deoxycholate, 0.2% Nonidet P-40, 0.1% SDS,

0.25 mM PMSF, and 10 mg/ml aprotinin). The lysate was incubated for 3 h at 4°C with purified anti-PPARα antibody. The immune complexes were precipitated with *Staphylococcus aureus* protein A bound to agarose beads. After the precipitates had been washed in RIPA buffer, the labeled proteins were resolved by 10% SDS-PAGE and visualized by autoradiography.

*Analysis of fatty acid uptake ability.* Assays for fatty acid uptake were carried out according to a method reported by Graulet et al. (52) with minor modifications. Briefly, 3 mice in each group were fasted overnight. Livers were removed quickly, rinsed in ice-cold saline solution, and cut into 500-μm thick slices with an Oxford Vibratome (Oxford Laboratories). Approximately 150 mg of fresh liver (6–8 liver slices) was placed on stainless steel grids positioned in a 25-ml flask equipped with suspended plastic center wells (Kontes) and incubated in RPMI-1640 medium (Sigma-Aldrich) devoid of fatty acids for 2 h at 37°C. The medium was then replaced with fresh RPMI-1640 medium supplemented with an antibiotic-antimycotic cocktail and 0.8 mM [1-$^{14}$C]palmitic acid (4 mCi/mmol) (American Radiolabeled Chemicals) complexed to BSA (palmitic acid:albumin molar ratio of 4:1). After a 7-h incubation, the medium was collected and slices were washed with 2 ml of saline solution and homogenized in Tris buffer (25 mM Tris-HCl, pH 8.0; 50 mM NaCl). Fatty acid uptake ability was calculated as the sum of palmitic acid converted to $CO_2$ and ketone bodies with that incorporated into total cellular lipids after incubation. For measurement of $CO_2$ production by the liver slices, the center wells were placed into scintillation vials containing 4 ml of scintillation cocktail, and radioactivity was counted. For measurement of ketone body generation, aliquots of medium (500 μl) and liver homogenates (250 μl) were treated with ice-cold perchloric acid to make final concentrations of 200 mM and were centrifuged at 3,000 *g* for 20 min at 4°C. Aliquots of the supernatant containing the ketone bodies were introduced into the scintillation vials, and radioactivity was counted. Total cellular lipids were extracted from the liver homogenates according to a modified method developed by Folch et al. (53), collected into scintillation vials, and evaporated to dryness under an air stream; radioactivity was then counted. The experiment was repeated 3 times, and palmitic acid uptake ability was expressed as fold changes relative to that of *Ppara*$^{+/+}$ nontransgenic mice.

*Other methods.* To determine the hepatic content of lipids and lipid peroxides, lipids were extracted according to a method by Folch et al. (53). Triglycerides and free fatty acids were measured with a Triglyceride E-test kit and a NEFA C-test kit (Wako), respectively. Lipid peroxides (malondialdeyde and 4-hydroxyalkenals) were measured using an LPO-586 kit (OXIS International). Hepatic β-oxidation activity was determined as described previously (16). Hepatic caspase 3 activity was measured as described elsewhere (54). Plasma glucose and insulin levels were determined using a Glucose CII-test kit (Wako) and a mouse insulin ELISA kit (U-type, AKRIN-031; Shibayagi), respectively.

*Statistics.* Statistical analysis was performed with a 2-tailed Student's *t* test for quantitative variables or with a chi-square test for qualitative variables. Quantitative data are expressed as the mean ± SD. $P < 0.05$ was considered to be statistically significant.

## Acknowledgments

We thank Trevor Ralph for editorial assistance and Chikako Tanaka for helpful suggestions.

Received for publication August 13, 2007, and accepted in revised form November 7, 2007.

Address correspondence to: Naoki Tanaka, Department of Metabolic Regulation, Institute on Aging and Adaptation, Shinshu University Graduate School of Medicine, Asahi 3-1-1, Matsumoto 390-8621, Japan. Phone: 81-263-37-2850; Fax: 81-263-37-3094; E-mail: naopi@hsp.md.shinshu-u.ac.jp.

1. Kiyosawa, K., et al. 1990. Interrelationship of blood transfusion, non-A, non-B hepatitis and hepatocellular carcinoma: analysis by detection of antibody to hepatitis C virus. *Hepatology.* **12**:671–675.
2. Kiyosawa, K., et al. 2004. Hepatocellular carcinoma: recent trends in Japan. *Gastroenterology.* **127**(5 Suppl. 1):S17–S26.
3. Tanaka, Y., et al. 2002. Inaugural article: a comparison of the molecular clock of hepatitis C virus in the United States and Japan predicts that hepatocellular carcinoma incidence in the United States will increase over the next two decades. *Proc. Natl. Acad. Sci. U. S. A.* **99**:15584–15589.
4. Okuda, K., Fujimoto, I., Hanai, A., and Urano, Y. 1987. Changing incidence of hepatocellular carcinoma in Japan. *Cancer Res.* **47**:4967–4972.
5. El-Serag, H.B., and Mason, A.C. 1999. Rising incidence of hepatocellular carcinoma in the United States. *N. Engl. J. Med.* **340**:745–750.
6. Shimotohno, K. 2000. Hepatitis C virus and its pathogenesis. *Semin. Cancer Biol.* **10**:233–240.
7. Moriya, K., et al. 1997. Hepatitis C virus core protein induces hepatic steatosis in transgenic mice. *J. Gen. Virol.* **78**:1527–1531.
8. Shintani, Y., et al. 2004. Hepatitis C virus infection and diabetes: direct involvement of the virus in the development of insulin resistance. *Gastroenterology.* **126**:840–848.
9. Moriya, K., et al. 1998. The core protein of hepatitis C virus induces hepatocellular carcinoma in transgenic mice. *Nat. Med.* **4**:1065–1068.
10. Powell, E.E., Jonsson, J.R., and Clouston, A.D. 2005. Steatosis: co-factor in other liver diseases. *Hepatology.* **42**:5–13.
11. Ohata, K., et al. 2003. Hepatic steatosis is a risk factor for hepatocellular carcinoma in patients with chronic hepatitis C virus infection. *Cancer.* **97**:3036–3043.
12. Browning, J.D., and Horton, J.D. 2004. Molecular mediators of hepatic steatosis and liver injury. *J. Clin. Invest.* **114**:147–152.
13. Le, T.H., et al. 2004. The zonal distribution of megamitochondria with crystalline inclusions in nonalcoholic steatohepatitis. *Hepatology.* **39**:1423–1429.
14. Yang, S., Lin, H.Z., Hwang, J., Chacko, V.P., and Diehl, A.M. 2001. Hepatic hyperplasia in noncirrhotic fatty livers: is obesity-related hepatic steatosis a premalignant condition? *Cancer Res.* **61**:5016–5023.
15. Desvergne, B., and Wahli, W. 1999. Peroxisome proliferator-activated receptors: nuclear control of metabolism. *Endocr. Rev.* **20**:649–688.
16. Aoyama, T., et al. 1998. Altered constitutive expression of fatty acid-metabolizing enzymes in mice lacking the peroxisome proliferator-activated receptor α (PPARα). *J. Biol. Chem.* **273**:5678–5684.
17. Staels, B., et al. 1998. Mechanism of action of fibrates on lipid and lipoprotein metabolism. *Circulation.* **98**:2088–2093.
18. Harano, Y., et al. 2006. Fenofibrate, a peroxisome proliferator-activated receptor α agonist, reduces hepatic steatosis and lipid peroxidation in fatty liver Shionogi mice with hereditary fatty liver. *Liver Int.* **26**:613–620.
19. Yeldandi, A.V., Rao, M.S., and Reddy, J.K. 2000. Hydrogen peroxide generation in peroxisome proliferator-induced oncogenesis. *Mutat. Res.* **448**:159–177.
20. Yu, S., Rao, M.S., and Reddy, J.K. 2003. Peroxisome proliferator-activated receptors, fatty acid oxidation, steatohepatitis and hepatocarcinogenesis. *Curr. Mol. Med.* **3**:561–572.
21. Peters, J.M., Cattley, R.C., and Gonzalez, F.J. 1997. Role of PPARα in the mechanism of action of the nongenotoxic carcinogen and peroxisome proliferator Wy-14,643. *Carcinogenesis.* **18**:2029–2033.
22. Fan, C.Y., et al. 1998. Steatohepatitis, spontaneous peroxisome proliferation and liver tumors in mice lacking peroxisomal fatty acyl-CoA oxidase. Implications for peroxisome proliferator-activated receptor α natural ligand metabolism. *J. Biol. Chem.* **273**:15639–15645.
23. Moriya, K., et al. 2001. Oxidative stress in the absence of inflammation in a mouse model for hepatitis C virus-associated hepatocarcinogenesis. *Cancer Res.* **61**:4365–4370.
24. Lee, S.S., et al. 1995. Targeted disruption of the α isoform of the peroxisome proliferator-activated receptor gene in mice results in abolishment of the pleiotropic effects of peroxisome proliferators. *Mol. Cell. Biol.* **15**:3012–3022.
25. Mandard, S., Muller, M., and Kersten, S. 2004. Peroxisome proliferator-activated receptor α target genes. *Cell. Mol. Life Sci.* **61**:393–416.
26. Peters, J.M., et al. 1998. Role of peroxisome proliferator-activated receptor α in altered cell cycle regulation in mouse liver. *Carcinogenesis.* **19**:1989–1994.
27. Tsutsumi, T., et al. 2002. Interaction of hepatitis C virus core protein with retinoid X receptor α modulates its transcriptional activity. *Hepatology.* **35**:937–946.
28. Tanaka, N., et al. 2003. In vivo stabilization of nuclear retinoid X receptor α in the presence of peroxisome proliferator-activated receptor α. *FEBS Lett.* **543**:120–124.
29. Moriishi, K., et al. 2007. Critical role of PA28γ in hepatitis C virus-associated steatogenesis and hepatocarcinogenesis. *Proc. Natl. Acad. Sci. U. S. A.* **104**:1661–1666.
30. Perlemuter, G., et al. 2002. Hepatitis C virus core

protein inhibits microsomal triglyceride transfer protein activity and very low density lipoprotein secretion: a model of viral-related steatosis. *FASEB J.* **16**:185–194.
31. Korenaga, M., et al. 2005. Hepatitis C virus core protein inhibits mitochondrial electron transport and increases reactive oxygen species (ROS) production. *J. Biol. Chem.* **280**:37481–37488.
32. Gomez-Gonzalo, M., et al. 2004. Hepatitis C virus core protein regulates p300/CBP co-activation function. Possible role in the regulation of NF-AT1 transcriptional activity. *Virology.* **328**:120–130.
33. Yu, S., and Reddy, J.K. 2007. Transcription coactivators for peroxisome proliferator-activated receptors. *Biochim. Biophys. Acta.* **1771**:936–951.
34. Spaziani, A., Alisi, A., Sanna, D., and Balsano, C. 2006. Role of p38 MAPK and RNA-dependent protein kinase (PKR) in hepatitis C virus core-dependent nuclear delocalization of cyclin B1. *J. Biol. Chem.* **281**:10983–10989.
35. Diradourian, C., Girard, J., and Pegorier, J.P. 2005. Phosphorylation of PPARs: from molecular characterization to physiological relevance. *Biochimie.* **87**:33–38.
36. Reddy, J.K., Rao, M.S., Azarnoff, D.L., and Sell, S. 1979. Mitogenic and carcinogenic effects of a hypolipidemic peroxisome proliferator, [4-chloro-6-(2,3-xylidino)-2- pyrimidinylthio]acetic acid (Wy-14,643), in rat and mouse liver. *Cancer Res.* **39**:152–161.
37. Rao, M.S., and Reddy, J.K. 1996. Hepatocarcinogenesis of peroxisome proliferators. *Ann. N. Y. Acad. Sci.* **804**:573–587.
38. Genini, D., and Catapano, C.V. 2006. Control of peroxisome proliferator-activated receptor fate by the ubiquitin-proteasome system. *J. Recept. Signal. Transduct. Res.* **26**:679–692.
39. Dharancy, S., et al. 2005. Impaired expression of the peroxisome proliferator-activated receptor alpha during hepatitis C virus infection. *Gastroenterology.* **128**:334–342.
40. de Gottardi, A., et al. 2006. Peroxisome proliferator-activated receptor-alpha and -gamma mRNA levels are reduced in chronic hepatitis C with steatosis and genotype 3 infection. *Aliment. Pharmacol. Ther.* **23**:107–114.
41. Lefkowitch, J.H., et al. 1993. Pathological diagnosis of chronic hepatitis C: a multicenter comparative study with chronic hepatitis B. *Gastroenterology.* **104**:595–603.
42. Moriya, K., et al. 2001. Increase in the concentration of carbon 18 monounsaturated fatty acids in the liver with hepatitis C: analysis in transgenic mice and humans. *Biochem. Biophys. Res. Commun.* **281**:1207–1212.
43. Barbaro, G., et al. 1999. Hepatocellular mitochondrial alterations in patients with chronic hepatitis C: ultrastructural and biochemical findings. *Am. J. Gastroenterol.* **94**:2198–2205.
44. Hui, J.M., et al. 2003. Insulin resistance is associated with chronic hepatitis C virus infection and fibrosis progression [corrected]. *Gastroenterology.* **125**:1695–1704.
45. Kato, J., et al. 2001. Normalization of elevated hepatic 8-hydroxy-2′-deoxyguanosine levels in chronic hepatitis C patients by phlebotomy and low iron diet. *Cancer Res.* **61**:8697–8702.
46. Horiike, S., et al. 2005. Accumulation of 8-nitroguanine in the liver of patients with chronic hepatitis C. *J. Hepatol.* **43**:403–410.
47. Takenaka, K., et al. 1994. Possible multicentric occurrence of hepatocellular carcinoma: a clinicopathological study. *Hepatology.* **19**:889–894.
48. Oikawa, T., et al. 2005. Multistep and multicentric development of hepatocellular carcinoma: histological analysis of 980 resected nodules. *J. Hepatol.* **42**:225–229.
49. Akiyama, T.E., et al. 2001. Peroxisome proliferator-activated receptor-α regulates lipid homeostasis, but is not associated with obesity. *J. Biol. Chem.* **276**:39088–39093.
50. Nakajima, T., et al. 2004. Peroxisome proliferator-activated receptor α protects against alcohol-induced liver damage. *Hepatology.* **40**:972–980.
51. Ni, R., et al. 1994. Fas-mediated apoptosis in primary cultured mouse hepatocytes. *Exp. Cell Res.* **215**:332–337.
52. Graulet, B., Gruffat, D., Durand, D., and Bauchart, D. 1998. Fatty acid metabolism and very low density lipoprotein secretion in liver slices from rats and preruminant calves. *J. Biochem.* **124**:1212–1219.
53. Folch, J., Lees, M., and Sloane Stanley, G.H. 1957. A simple method for the isolation and purification of total lipids from animal tissues. *J. Biol. Chem.* **226**:497–509.
54. Gurtu, V., Kain, S.R., and Zhang, G. 1997. Fluorometric and colorimetric detection of caspase activity associated with apoptosis. *Anal. Biochem.* **251**:98–102.

ELSEVIER

Journal of Hepatology 48 (2008) 858–879

Journal of Hepatology

www.elsevier.com/locate/jhep

Review

# Experimental models of hepatocellular carcinoma☆

Philippa Newell[1,2], Augusto Villanueva[1], Scott L. Friedman[1], Kazuhiko Koike[3], Josep M. Llovet[1,4,*]

[1]*Division of Liver Diseases, Mount Sinai School of Medicine, 1425 Madison Avenue, Box 1123, New York, NY 10029, USA*
[2]*Department of Surgery, Mount Sinai School of Medicine, 1425 Madison Avenue, Box 1123, New York, NY 10029, USA*
[3]*Department of Infectious Diseases, Internal Medicine, Graduate School of Medicine, University of Tokyo, Japan*
[4]*BCLC Group, Liver Unit, IDIBAPS, CIBERehd, Hospital Clínic, Barcelona, Spain*

**Hepatocellular carcinoma (HCC) is a common and deadly cancer whose pathogenesis is incompletely understood. Comparative genomic studies from human HCC samples have classified HCCs into different molecular subgroups; yet, the unifying feature of this tumor is its propensity to arise upon a background of inflammation and fibrosis. This review seeks to analyze the available experimental models in HCC research and to correlate data from human populations with them in order to consolidate our efforts to date, as it is increasingly clear that different models will be required to mimic different subclasses of the neoplasm. These models will be instrumental in the evaluation of compounds targeting specific molecular pathways in future preclinical studies.**



*Keywords*: **Liver cancer; Hepatocellular carcinoma; Mouse models; Genetically engineered mice; Cirrhosis**

## 1. Introduction

Hepatocellular carcinoma is one of the world's deadliest cancers, ranking third among all cancer-related mortalities. Most cases occur in Asia and sub-Saharan Africa, where viral hepatitis is endemic. The incidence is rising in the West, likely due to the increase in patients infected with hepatitis C during the latter half of the last century [1]. The liver, unique in its capacity for regeneration following injury, also gives rise to this malignancy commonly associated with the inflammatory state of advanced fibrosis, or cirrhosis. Potentially curative therapies can be offered to approximately 30% of patients, but are complicated by a high rate of recurrence [2].

Encouraging progress has been made in understanding the molecular pathogenesis of cancer [1,2]. The discoveries of the signal transduction pathways, cascades of protein–protein interactions transmitting information from the cell surface to the nucleus, and of their link to tumor biology, are particularly impressive.

Several key mouse models have been instrumental in defining the pathogenesis of HCC by introducing genetic

*Associate Editor: M. Colombo*

☆ P. Newell is a recipient of an American Liver Foundation (ALF) Postdoctoral Research Fellowship Award (2007). A. Villanueva is supported by grants from the Fundación Caixa Galicia and the National Cancer Center. S. Friedman is a Professor of Medicine and Chief of the Division of Liver Diseases, supported by NIH Grant number DK37340. K. Koike is Chairman of Department of Infectious Diseases, University of Tokyo, supported by grant from the Ministry of Health, Labor and Welfare, and Ministry of Education, Science, Sports and Culture of Japan. J.M. Llovet is Director of the HCC Program in Mount Sinai and Professor of Research-ICREA in the Hospital Clínic Barcelona, supported by National Institute of Health-NIDDK grant 1R01DK076986-01, National Institute of Health-I+D Program (Spain) grant number SAF-2007-61898. The authors declare that they do not have anything to disclose regarding funding from industries or conflict of interest with respect to this manuscript.

* Corresponding author. Address: Division of Liver Diseases, Mount Sinai School of Medicine, 1425 Madison Avenue, Box 1123, New York, NY 10029, USA. Tel.: +1 212 659 9503; fax: +1 212 849 2574.
*E-mail address:* josep.llovet@mssm.edu (J.M. Llovet).

*Abbreviations:* HCC, hepatocellular carcinoma; HCV, hepatitis C virus; TKR, tyrosine kinase receptor; HBV, hepatitis B virus; TSG, tumor suppressor gene; TSP, tissue specific promoter; Tg, transgene.

0168-8278/$32.00 © 2008 European Association for the Study of the Liver. Published by Elsevier B.V. All rights reserved.
doi:10.1016/j.jhep.2008.01.008

alterations into one or more aetiologic pathways that can be targeted exclusively to the liver. Moreover, these programmed manipulations can be introduced systematically, not only in this specific organ but also at defined times during development, growth and aging of the liver.

Nonetheless, substantial challenges persist in modeling liver diseases whose natural history requires a chronic inflammatory milieu. For example, infectious (hepatitis C virus), toxic (alcohol), metabolic (non-alcoholic steatohepatitis), or congenital (hemachromatosis) diseases share inflammation and fibrosis as precursors to cancer, yet none is easily mimicked in animals. There are few rodent models of HCC arising spontaneously within a background of regenerative nodules and cirrhosis, and most depend on the administration of hepatotoxic and/or carcinogenic agents to recreate the injury–fibrosis–malignancy cycle seen in chronic human liver diseases.

Comparative genomic studies in human HCC samples have begun to identify molecular subgroups with characteristic mutations, gene expression profiles and chromosomal gains and losses [3]. Moreover, since there is no single dominant molecular pathology underlying all HCCs, it is increasingly clear that different models will be required to mimic different subclasses of the neoplasm. These models will be instrumental as pre-clinical tools to evaluate compounds targeting specific molecular pathways.

With these challenges in mind, the objective of this review is to assemble and evaluate the available models of both cirrhosis and HCC, to provide a blueprint for understanding the pathogenesis of HCC and for optimizing preclinical models for drug testing.

## 2. Experimental models in cancer research

Although many experiments focusing on liver physiology have been conducted in rats due to their propensity for the development of fibrosis, the laboratory mouse (*Mus musculus*) is considered among the best model systems for cancer because of the availability of gene targeting methods, as well as the animal's size and breeding capacity, its lifespan of 3 years, and its physiologic and molecular similarities to human biology [4]. Significant advances have been made in modeling cancer genetics in mice, along a spectrum that ranges from simple xenograft models to more complex, genetically modified mice. Examples of each of the following are illustrated in Table 1.

### 2.1. Xenograft models

The demonstration that concentrated cancer cells grown *in vitro* could form tumors when implanted subcutaneously into an immunocompromised mouse was first established in 1969 [5]. This xenograft model has since demonstrated several advantages that explain its persistence as the mainstay of pre-clinical studies of anti-neoplastic drugs *in vivo*: the tumors are rapidly and easily induced, and their subcutaneous location enables direct measurement of tumor growth. More recently, however, several critical differences between xenograft- and patient-derived specimens have become apparent, as discussed below. In addition, cancer is now appreciated as a complex disease dependent upon the interaction between transformed cells harboring oncogenic mutations, referred to as the 'cell autonomous compartment', and their surrounding tumor environment, the 'non-cell autonomous constituents' made up of normal cells, stromal cells, and immune cells [4], features that are not part of the xenograft approach.

Mouse models of cancer were first introduced over 60 years ago. Shortly after its inception in 1955, the Developmental Therapeutics Program at the National Cancer Institute (NCI) adopted the use of three transplanted rodent models of sarcoma, carcinoma, and leukemia, for the purposes of selecting agents for clinical use in cancer patients. Thousands of molecules were tested in mice bearing murine leukemias during the first decades of modern cancer drug development, circa 1945–1969 [6]. This tumor panel was later expanded to include human tumor xenografts, with the intention to study drug activity against solid tumors [7]. In 1990, the NCI focused on the development of *in vitro* assays in 60 different cell lines in order to screen pharmaceutical agents for their potency and their selective activity against either a particular disease category or specific cell line [8,9], the most promising of which were to be subsequently evaluated in the nude mouse xenograft model.

The validity of xenografts as a predictive indicator of probable clinical activity is limited, with the most success seen in cytotoxic agents. A retrospective analysis performed by the NCI for 39 compounds in which both xenograft testing and Phase II clinical data were available showing that less than 50% of agents with activity in more than one-third of xenografts showed clinical activity ($p = 0.04$) [6]. The same study demonstrated that activity in a particular histology in a tumor model did not closely correlate with activity in the same human cancer histology [10], with the exception of non-small cell lung and ovarian cancer [11].

There are several variables inherent to the xenograft experiments which may impact on the divergent outcomes compared to human disease, including growth properties and size at initiation of treatment of xenograft tumor, ectopic versus orthotopic location of tumor, local versus metastatic disease [12], tolerance for high doses of chemotherapeutic agents in mice [13],

**Table 1**
**Available mouse models in cancer research**

| | Technical Method | Advanced Mouse Models of Cancer | Current Models in HCC | Future Prospects: Wish List for HCC |
|---|---|---|---|---|
| Xenograft | Xenograft  | COLON, BREAST, PROSTATE: Surgical orthotopic implantation: intact fragments of human cancer, including tumors taken directly from the patient, transplanted into the corresponding organ of immunodeficient rodents[16] | Orthotopic xenograft model in which hepatoma 129 cells originating from C3H mice are injected into fibrotic livers of mice pretreated with TAA and EtOH[40] | Mouse HCC cell line derived from GEM tumor with specific molecular pathway dysregulated, with immunofluorescent marker, injected into fibrotic liver of immune-competent mice |
| Transgenic GEM | Constitutive Transgenic 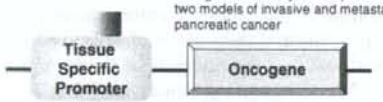  | PANCREATIC: $Kras^{G12V}$ and chronic pancreatitis[188]; $Trp53^{R172H}$ and $Kras^{G12D}$ double transgenic driven by insulin promoter[170]; two models of invasive and metastatic pancreatic cancer | Mouse C-myc/Human E2F-1 overexpression driven by albumin promoter[171]; HCC at 6-8 months | Double transgenic overexpressing profibrotic gene combined with liver-specific oncogene |
| | Dominant Negative Transgenic 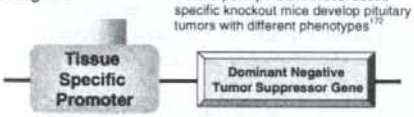  | PITUITARY: Rb and p27Kip1 Cdk inhibitor tissue specific knockout mice develop pituitary tumors with different phenotypes[172] | Mdr-2 knockout mice are unable to secrete phospholipids into bile, and develop cholangitis and HCC at 6-12 months[166] | Double transgenic liver-specific E-cadherin knockout and β-catenin overexpression |
| | Inducible Transgenic 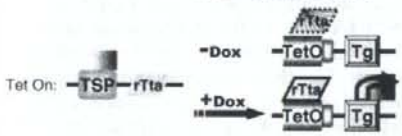  | MELANOMA: Double transgenic combining Tet-induced overexpression of mutated $Hras^{V12G}$ and Ink4a knockout[179] | Tet-inducible Met expression under albumin promoter: 60% HCC at 12 months; tumors regressed when transgene (Tg) was inactivated[91] 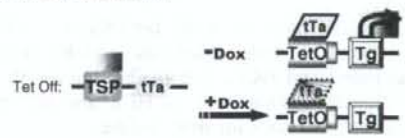  | Tet-induced, liver-specific overexpression of known oncogene in fibrotic mice |
| Endogenous GEM | Conditional Gene Targeting 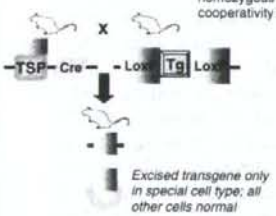  | PROSTATE: Double transgenic Cre-mediated $PTEN^{-/-}$ homozygous loss and $p19Arf^{+/-}$: cooperativity in cancer development[174] | Cre-mediated liver specific PTEN-/- knockout: 66% HCC at 8 months[108] | Cre-mediated, liver-specific knockout of known tumor suppressor gene in fibrotic mice |

and variability in selected endpoints. These variables can be minimized if given due consideration in the design of preclinical cancer drug experiments. However, the greatest discrepancies between success of cancer therapies in xenograft models and in human clinical trials are likely due to critical differences in both the tumor cells and their microenvironment. Natural tumor progression is a micro-evolutionary process during which increasingly aggressive clones, generated through genetic instability, emerge from an initially monoclonal lesion. Autochthonous tumors, those that evolve *in situ* from normal cells, tend to have a diminished genetic heterogeneity compared to tumor xenografts, although selective pressures of cell culture or tissue explantation can cause a rapid expansion of a certain clonal constituent of polyclonal tumors [14,15].

One solution to this disparity between cancer cell lines and human tumors is surgical orthotopic implantation, in which intact fragments of human cancer taken directly from the patient are transplanted into the corresponding organ of immunodeficient rodents, as reviewed by Hoffman [16]. This technique has been applied to breast, lung, and prostate cancer among others.

Additional advances have been made in the xenograft model through the addition of mesenchymal stem cells to weakly metastatic cancer cell lines, which enhances the ability of the cell lines to form tumors and to metastasize [17]. Wu et al. were able to isolate a side population (SP) from 29 sarcomas which preferentially formed tumors when grafted into immunodeficient mice; only cells from tumors that developed from the SP cells had the ability to initiate tumor formation upon serial transplantation [18].

Our deepening appreciation of the non-cell autonomous constituents of the tumor microenvironment, including the stroma and immune cells relevant to liver pathology in particular, provides further evidence that the xenograft model is more appropriately termed *animal culture*, as suggested by Tuveson and Frese [4].

### 2.2. Genetically engineered mouse models (GEM)

The most sophisticated animal models of human cancer are those that have been genetically engineered to mimic the pathophysiological and molecular features of human malignancies [4]. Such models enable the investigation of a range of discrete molecular stages that occur during tumor progression both within tumor cells and within their microenvironment; additionally, mice harboring multiple mutations provide information regarding pathway cooperativity and dependency *in vivo* [19].

Despite these strengths, there are a number of important limitations in mouse models of cancer, such as variation in basic cellular processes, as well as in telomere length and telomerase expression [20,21]. It is also well documented that identical genetic lesions can produce different pathologies in mice than in humans [22]. GEM can be categorized as either transgenic or endogenous models.

### 2.3. Transgenic models

Transgenic mice are those that are engineered to express either oncogenes or dominant-negative tumor suppressor genes in a non-physiologic manner due to ectopic promoter and enhancer elements [4,19]. Microinjection of recombinant DNA directly into the pronucleus of a fertilized mouse egg is the classic method for generating transgenic mice [23], but transgenic mice can also be produced through gene targeting ("knock-in") and lentiviral transduction in embryonic stem cells.

Constitutive expression of cellular and viral oncogenes and germline disruptions of tumor suppressor genes were the first approaches used to create strains of cancer-prone mice [19,24]. The cDNA constructs can contain promoter elements designed to restrict tissue tropism, so although the effect of the oncogenic gain will be constitutive, its expression can be limited to specific tissues by the use of tissue-specific promoters [19], for example the albumin promoter in liver transgenic models.

Germline tumor suppressor cell mutant mice were initially developed to parallel human inherited cancer predisposition syndromes. However, although many of these heterozygous mice were tumor-prone and demonstrated loss of the wild-type allele in their tumors, few of them developed the clinical features of the cognate human syndrome. For example, loss of the retinoblastoma gene product Rb in humans leads to retinoblastomas, osteosarcomas, and small cell lung cancer; whereas Rb heterozygote mice develop thyroid and pituitary tumors but no retinoblastomas [25]. Rb heterozygotes are able to compensate for loss of Rb, a finding that highlights the existence of shared and predictable cellular process within both species [20,26]. So, although identical genetic lesions may not perfectly recapitulate the human disease in mice, there is no doubt that these genetically engineered mice are valuable tools for understanding the underlying biological mechanisms of tumorigenesis [22]. Their ability to recapitulate the genetic features of amplified proto-oncogenes, such as c-myc [27], has contributed greatly to our understanding of cancer biology.

There are, however, additional weaknesses of these models that have spurred the development of more advanced methods. For example, because the genes affected may be vital to normal development, overexpression or ablation may lead to embryonic lethality or infertility [24]. Promoter fragments typically represent the minimal sequence required for tissue-specific expression and do not necessarily allow the same control conferred by endogenous regulatory elements [28]; for example, a typical transgene would not include all transcription factor and microRNA binding sites [4,29]. And, although the DNA fragments are thought to associate by homologous recombination before integration and in most cases insert at a single chromosome site [23], there is little control over site of integration and copy number [22]. This can result in pronounced variability of expression patterns, as the exogenous gene can affect genes near its insertion site or can be affected by endogenous control elements [22,30–32]. Also, although conventional mouse mutants may be useful for modeling familial forms of cancer, they do not mimic sporadic tumorigenesis because the

initiating mutation is present in all cells of the body, including those that constitute the tumor microenvironment [33].

### 2.4. Inducible systems of oncogene expression

Bujard and colleagues developed a strategy for temporally controlled and reversible transgene expression, using a tetracycline (tet-) inducible system [34]. These drug- or ligand-inducible systems involve the use of a chimeric transcriptional activator that reversibly activates a target gene in response to the administration of the inducing agent.

The *Escherichia coli* tetracycline resistance operon has been applied widely to generate cell lines and murine models with tightly regulated gene expression in response to tetracycline [35]. The tet transactivator functions either as a constitutive repressor that is inducibly inhibited by ligand to allow expression from the *tet* operon (tTA), or it acts as an inducible activator of the *tet* operon upon ligand addition (rtTA) [19]. This system has been particularly useful to study the concept of oncogene addiction; nearly all oncogenes tested thus far seem to be required not only for tumor initiation, but also for tumor maintenance [33].

### 2.5. Endogenous GEM: knock-out models

Endogenous GEM are those that lose the expression of tumor suppressor genes (TSG) or that express dominant-negative tumor suppressor genes or oncogenes from their native promoters [4]. The original 'knockout' mouse model entailed disruption of an allele in endogenous embryonic stem cells using a targeting vector. Biallelic disruption of TSG often results in embryonic lethality, but heterozygous mice can be used to determine the tumorigenic potential of the genes, such as the retinoblastoma tumor suppressor gene (Rb) [25]. These germline mutations are present throughout the mouse and are constitutively expressed, unlike the sporadic mutations occurring in human tumors that are surrounded by normal tissue.

### 2.6. Endogenous GEM: conditional gene targeting

As reviewed by Maddison et al. [22], model systems have now been developed which allow both spatial and temporal control of gene expression. These are predominantly dependent on the creation of bi-transgenic mice: those carrying a tissue-specific, inducible transactivator gene are crossed to mice carrying the allele of interest which has been engineered to be controlled by the transactivator. Offspring that carry both transgenic elements are treated with the inducer to express the transactivator gene in a specific tissue, which then acts on the desired allele. This system requires the exogenous delivery of the cre gene (usually by an adeno- or retrovirus), and the induction is irreversible.

Conditional inactivation of tumor suppressor genes relies on the ability of a viral or prokaryotic site-specific recombinase to recognize a pair of target DNA sequences and catalyze recombination at these sites, which results in either deletion or inversion of the intervening DNA sequence [19]. A commonly used tool is the Cre-Lox system, wherein Cre (*C*auses *re*combination) recombinase, isolated from bacteriophage P1, catalyses site-specific recombination between defined 34 bp Lox P sites (*Lo*cus $\chi$ of crossover *P*1) [36,37]. If gene $\chi$ is placed between two Lox P sites and then exposed to Cre, it will be excised, or 'floxed out'. An alternative system to Cre-Lox uses the FLP recombinase, which recognizes the 48 bp Frt site [38]. Transgenic mice that express recombinase from a specific promoter are bred to mice carrying conditional tumor suppressor gene mutations, so that the TSG can be bi-allelically inactivated to allow the generation of organ- and cell-lineage-specific tumors models [19].

Conditional activation of oncogenes is created by the insertion of a LoxP flanked transcriptional silencing element between the promoter and the mutant oncogene-encoding sequence. Conditional oncogenes are constructed using classic transgenic technology, but expression of the oncogene is only activated by the recombinase-mediated removal of the transcriptional silencer. This allows for tissue-specific oncogene expression [39].

This second generation of GEM, which more faithfully recapitulates sporadic tumor formation by the induction of somatic mutations in a time- and tissue-specific fashion, has provided great insight into the contribution of genes in the initiation, progression, and treatment of cancer. We will now discuss how each of these systems has been used to further our understanding of liver cancer.

## 3. Experimental models of hepatocellular cancer

Hepatocellular carcinoma universally arises upon a background of inflammation and fibrosis. Creation of animal models of HCC presents a particular experimental challenge because of the difficulty in modeling chronic inflammation without using carcinogens to induce liver injury, and because of the heterogeneity of molecular pathways that are dysregulated during this transition from cirrhosis to cancer.

HCC is preceded in both rodents and humans by the development of premalignant lesions including foci of altered hepatocytes and dysplastic nodules, which exhibit a higher risk of malignant evolution than normal cells [40,41]. Various genetic alterations and exposures to chemical carcinogens have been studied in animals

in order to recapitulate the phenotypic, biological, and molecular events that occur during this transformation.

### 3.1. Xenograft models of HCC

In a recent attempt to characterize primary human xenografts in liver cancer, seven different primary HCC cell lines were injected into SCID mice. The mice were then treated with common chemotherapeutic agents such as cisplatin and gefitinib. There were significant differences in tumor growth inhibition between xenografts, which reinforced the concern for high internal variability of this model in human cancer. Interestingly, the study concluded that most of the chemotherapeutic agents currently used in the treatment of HCC have little or no anti-neoplastic activity in these models [42].

Ma et al. have examined HCC cells expressing CD133 [43], which exhibit stem cell properties and are chemoresistant: purified CD133(+) HCC cells isolated from human HCC cell lines and harvested from xenograft mouse models survived chemotherapy in increased proportions relative to most tumor cells which lack the CD133 phenotype [44]. The inclusion of stem cell-enriched HCC cell lines will likely enhance future preclinical studies in HCC therapeutics (see Table 1).

A group of investigators at the University Hospital Bonn created an orthotopic xenograft model in which hepatoma 129 cells originating from C3H mice were injected into fibrotic livers of mice pretreated with thioacetamide by intraperitoneal injection and alcohol per oral [45]. They found that tumors in fibrotic livers grew significantly larger and more rapidly than those in normal livers, and were able to metastasize and form satellite nodules. Gene expression analysis revealed greater intratumoral expression of vascular endothelial growth factor (VEGF) and its receptor (VEGFR), and of MMP-2 and MMP-9 in the fibrotic liver tumors. This useful model provides a unique tool for testing drug efficacy in orthotopic hepatoma xenograft within the context of liver fibrosis.

### 3.2. Viral models of HCC

Infection causing latent or chronic viral hepatitis is the most common aetiology of HCC, comprising 80% of cases worldwide. Hepatitis B virus (HBV) is endemic in China, Southeast Asia, and sub-Saharan Africa; there, vertical transmission of the virus results in high rates of HCC. Hepatitis C (HCV) viral infection is more prevalent in the United States and Europe than either HBV or HIV [46]. The woodchuck hepatitis virus (WHV) induces a liver inflammation, injury and repair process in woodchucks similar to those of HBV-positive patients and has therefore proven to be a useful model of the disease.

#### 3.2.1. Hepatitis B virus

HBV is a DNA virus that causes acute and chronic hepatocyte injury, inflammation, and HCC. During prolonged infection, viral DNA sequences integrate into the host cell genome, where they and the flanking cellular sequences are commonly rearranged [47], a phenomenon that can activate an adjacent cellular oncogene. In addition, viral infection can induce hepatocyte injury mediated by the antiviral cellular immune response and, to a lesser extent, by direct injury to the cells. Although most cases of HBV-associated HCC arise in a background of inflammation and fibrosis, the virus is notorious for also causing HCC in the absence of cirrhosis, most likely by integrating into the host chromosome and thereby promoting transcriptional transactivation of mitogenic factors.

The HBV virus is a circular DNA molecule containing four open reading frames encoding four HB viral proteins: preS/S, preC/C, P and X protein (HBx). The most common viral marker in HCC is the integration of HBV genomic DNA encoding HBx. In 1994, Koike et al. published their description of a transgenic mouse model demonstrating that high levels of HBx expression were sufficient to generate HCC in 84% of male transgenic mice at age 13–24 months [48] (see Table 2). Analysis of proliferation and DNA content in these mice suggested that the continued expression of HBx gene initiated tumor formation by inducing DNA synthesis and placing large numbers of hepatocytes subjective to secondary events for transformation [48]. Yu et al. also confirmed the development of HCC in HBx transgenic mice [49]. Although another research group did not see spontaneous HCC development, those HBx transgenic mice were more susceptible to chemical carcinogenesis than control mice [50]. The reason for this discrepancy is unclear, but the difference in genotype of HBV should be noted: HCC tumors arose in genotype C HBx transgenic mice but not in other genotypes [51].

Chisari et al. described a transgenic model that overproduces the hepatitis B virus large envelope polypeptide and accumulates toxic quantities of hepatitis B surface antigen (HBsAg) [52]. This hepatocellular injury initiates a programmed response within the liver, characterized by inflammation, regenerative hyperplasia, transcriptional deregulation, aneuploidy and eventually HCC. Inappropriate expression of a single structural viral gene was thereby shown to be sufficient to cause malignant transformation. The process of oncogenesis seen in this model also supports the theory that severe, prolonged cellular injury can induce a proliferative response that fosters secondary genetic events that lead to unrestrained growth [47]. However, the level of viral protein expression in this model may well surpass the expression in human infection.

**Table 2**
**Genetically engineered models of hepatocellular carcinoma**

| Gene | Type of mutation or tissue promoter/construct | Phenotype (+/− and −/−) | Chemically induced/ metastasis | References |
|---|---|---|---|---|
| *Viral models* | | | | |
| Hepatitis B virus large envelope protein | BglII-A fragment of HBV encoding large envelope protein under control of albumin promoter and enhancer | Focal necrosis, inflammation, and subsequent HCC in 72% males | No metastases; rare local invasion | [47,52] |
| Hepatitis B virus X protein | EcoRI–BglII fragment of HBV including the X gene under its own promoter and enhancer | HCC in 84% after 13–24 months in mice with high HBx expression | Lung metastasis | [48,175,176] |
| Hepatitis C virus | HCV core-E1–E2 transgenic under albumin promoter and HCV core transgenic under HBV X promoter | No DEN: No HCC in either strain by 21 months. +DEN: 100% HCC at 32 weeks; HCV core-E1–E2 with largest tumors ($p = 0.008$) | DEN injected weekly × 6 weeks | [56] |
| Hepatitis C virus | HCV core under HBV X promoter; HCV E1–E2 under HBV X promoter | Core transgenics: 32% HCCs in male mice at 16–23 months; E1–E2 transgenics: no HCC. No evidence hepatitis | None reported | [56,59] |
| Hepatitis C virus | HCV core-E1–E2 transgenic under albumin promoter and the entire HCV transgenic under albumin promoter | HCC in core-E1–E2 transgenic and entire HCV transgenic after 13 months | None reported | [60] |
| *Cell cycle models* | | | | |
| p53 germline knockout and liver-specific viral receptor TVA, injected with PyMT oncogene | p53 germline knockout [177] crossed with mice expressing viral receptor TVA under albumin promoter (Alb-TVA), injected at age 3 days intrahepatically with mouse polyoma virus middle T antigen | HCC in 42% of p53 null mice, in 37% of $p53^{+/-}$, and in 66% of $p53^{+/+}$ mice expressing TVA injected with PyMT at 4 months. No TVA-negative littermates developed HCC | Metastases in p53 null mice (6/16); less in $p53^{+/-}$ (1/14) | [67,177] |
| Trp53 and INK4a/ARF conditional mutant mice, injected with PyMT oncogene | Albumin Cre mice crossed with Trp53 conditional mutant and INK4a/ARF conditional mutant, injected at age 3 days intrahepatically with mouse polyoma virus middle T antigen | >90% HCC in combined Trp53, INK4a/ARF null mice injected with PyMT compared to single null gene | Metastases in Trp53 null mice (30%) and in combined Trp53, INK4a/ARF mice (63%) at 6 months | [68] |
| P53 conditional expression | Hepatoblasts transduced with oncogenic ras (Hras V12) and a tet-responsive P53 miRNA design short hairpin RNA | Complete tumor regressions when endogenous p53 reactivated in p53-deficient tumors | None reported | [69] |
| c-myc | c-myc over-expression under albumin enhancer/promoter [74,90,178,179]; under α1 antitrypsin promoter [180,181] | 15 weeks: polyploidy cells, dysplasia >60% [179]; 15 mos: 91% adenomas [74,178]; 54% HCC [178,180,181]; | None reported | [74,90,178–181] |
| c-myc and E2F-1 | Mouse c-myc and human E2F-1 over-expression under albumin promoter | 6–8 mos: 100% HCC [171,178] | None reported | [90,171,178,179] |
| c-myc and TGFα | c-myc over-expression under albumin enhancer/promoter; TGFα over-expression under metallothionein 1 promoter | 4 mos: 70% dysplastic nodules; 18% HCC [90] | Zinc in $H_2O$ accelerated nodule formation by 6–8 weeks | [90,182] |

(*continued on next page*)

**Table 2 (*continued*)**

| Gene | Type of mutation or tissue promoter/construct | Phenotype (+/− and −/−) | Chemically induced/ metastasis | References |
|---|---|---|---|---|
| SV40 T-antigen conditional and inducible expression | SV40 T-antigen expression under albumin enhancer/ promoter [74]; under major urinary protein enhancer/ promoter [183]; under metallothionein 1 promoter [184]; under α1 antitrypsin promoter [185]; under antithrombin III promoter [186]; tetracycline-inducible expression: mice expressing tTa under albumin promoter crossed with mice expressing T antigen under tTa promoter [75] | 3–7 mos: adenomas and HCC [74]; 10–12 weeks: HCC[185]; after 4–6 weeks: 100% HCC [186] | Lung metastases [186] | [74,75,181,183–186] |
| E2F-1 | E2F-1 over-expression under control of albumin enhancer/ promoter | 10 mos: 100% adenomas and dysplastic nodules; 12 mos: 33% HCC | None reported | [71,90,179] |
| *Telomere dysfunction models* | | | | |
| mTERT $^{-/-}$ and p53$^{+/-}$ or WT | Germline mTERT and p53 knockout over several generations and $CCl_4$ liver injury | 50 weeks: 100% HCC in p53$^{+/-}$ both generations (G0 and G3/ G4); 44% in wild-type G0 versus 9% HCC in wild-type G3/G4 | $CCl_4$ by IP injection 3×/ week × 4 months | [66] |
| *Pathway specific models* | | | | |
| Wnt/β-catenin | | | | |
| Activating mutation in β-catenin: truncated $NH_2$ terminal transgenic | EAB/9K/Δ N131 β-catenin construct under control of liver-specific enhancer of aldorase B gene (expressed throughout embryonic and post-natal development) | Death at 3 weeks from hepatomegaly; no dysplastic foci in liver | N/A | [127] |
| Activating mutation in β-catenin: exon 3 conditional knockout | Catnb$^{lox(ex3)}$ knockout and fatty acid binding protein Fabpl-cre transgenic | Death at 5 weeks from liver damage/mitochondrial swelling. No dysplastic foci in liver; +intestinal polyps | N/A | [128] |
| Activating mutation in β-catenin: exon 3 conditional knockout | Catnb$^{lox(ex3)}$ knockout injected with recombinant adenovirus expressing Cre from human CMV promoter | High multiplicity injection ($10^9$ pfu/mouse): death at 3 weeks with hepatomegaly/ mitochondrial swelling. Low multiplicity injection ($10^{7-8}$ pfu/ mouse): No dysplastic foci in liver >6 mos | N/A | [128] |
| β-catenin exon 3 knockout and activated H-ras (H-ras$^{G12V}$) double-transgenic conditional | Catnb$^{lox(ex3)}$ knockout and H-ras (Tg$^{lox(pA)H\text{-}ras^*}$) double-transgenic with recombinant adenovirus expressing Cre from human CMV promoter | Low multiplicity infection ($10^8$ pfu/mouse): 100% HCC at 6 months | Intrahepatic invasion | [131] |
| APC knockout liver-specific | Apc$^{\Delta ex14}$ knockout (−/−) injected in tails with recombinant adenovirus expressing Cre (injections infected primarily and massively the liver) | High multiplicity infection ($10^9$ pfu/mouse): Death within 2 months and hepatomegaly. Lower multiplicity infection ($0.5 \times 10^9$ pfu/mouse): 67% HCC at 9 months. Apc$^{+/-}$ had no liver abnormalities | None reported | [130] |
| β-catenin wild-type | β-catenin over-expression under control of albumin enhancer/promoter | Hepatomegaly (15% increased liver/body weight ratio); no dysplastic nodules at 24 months | N/A | [129] |

**Table 2 (*continued*)**

| Gene | Type of mutation or tissue promoter/construct | Phenotype (+/− and −/−) | Chemically induced/ metastasis | References |
|---|---|---|---|---|
| *PI3K/Akt pathway* | | | | |
| PTEN $^{-/-}$ | Albumin cre/PTEN$^{lox/lox}$ | Steatohepatitis; Adenomas at 44 weeks and 66% HCC at 78 weeks [108]; HCC in 66% of males at 44 weeks and in 83% of males and 50% of females at 78 weeks [109] | Lung metastases | [108,109] |
| *Insulin growth factor pathway* | | | | |
| IGF2 transgenic | IGF2 over-expression under control of urinary protein promoter | HCC in <10% at 18–24 months; also lymphomas, sarcomas, and thyroid carcinomas | None reported | [187] |
| IGF2 knockout and TGFα transgenic | TGFα over-expression under metallothionein 1 promoter [86] crossed with IGF2 heterozygous knockout mice (paternal null allele; maternal wild-type, normally imprinted) | (1) IGF2$^{wt/wt}$: no HCC; 4% adenoma; (2) IGF2$^{+/-}$ : dwarves, normal liver phenotype; (3) TGFα × IGF2$^{wt/wt}$ and (4) TGFα + IGF2$^{wt/-}$ : 100% HCC at 18 months | None reported. Zinc in drinking water starting at age 10 months | [188] |
| *Epidermal growth factor pathway* | | | | |
| EGF transgenic | Double-transgenic of the liver construct Alb-DS4 that encodes autocrine growth factor IgEGF crossed with AAT-myc mice | EGF transgenic (Alb-DS4): mortality from HCC by age 7.1 months; EGF/myc double-transgenic: accelerated mortality to 4.4 months | | [115] |
| *Ras signaling* | | | | |
| H-ras | Mutant c-H-ras over-expression under albumin promoter | Hepatomegaly, lung tumors [74] | None reported | [74] |
| *HGF/c-Met and TGF-α* | | | | |
| HGF transgenic | Mouse HGF expression driven by metallothionein promoter [95]; by albumin promoter[189] | Hepatomegaly; >17 months: adenomas and rare HCCs [95]; rapid recovery after partial hepatectomy, no dysplasia [189] | Most animals not given zinc because transgene expression adequate | [95,189] |
| HGF over-expression +/− β-catenin conditional knockout | Hydrodynamic injection of plasmid containing HGF under CMV promoter (pCMV-HGF) into wild-type and into AFP-enhancer albumin promoter-Cre floxed β-catenin knockout mice | HGF over-expression: hepatomegaly and increased Wnt/β-catenin signaling; no dysplastic nodules. HGF over-expression in β-catenin knockout: no alterations in liver | N/A | [96] |
| HGF + c-myc | Double-transgenic mouse c-myc driven by albumin promoter/enhancer and human HGF driven by albumin regulatory elements | Inhibition of hepatocarcinogenesis by HGF in c-myc transgenic mice: 0% HCC in HGF/c-myc versus 60% HCC at 16 months in c-myc single transgenic, even with addition of phenobarbital | Phenobarbital | [97] |
| HGF + TGF-α | Double-transgenic mouse TGFα over-expression under metallothionein 1 promoter and human HGF driven by albumin promoter | Increased proliferation and c-myc expression in HGF over-expressing mice. Diminished hepatocarcinogenesis by HGF in TGFα transgenic mice: 33% (3/9 mice) HCC in HGF/ TGFα versus 60% (6/10) in TGFα single transgenic | None reported | [98] |
| Met transgenic | Tetracycline-inducible expressing human Met under liver-specific promoter crossed with mice expressing tetracycline transactivator under liver-specific liver activating protein (MET-TRE/LAP-tTA) [91,99] | 12 months: 60% HCC; tumors regressed when transgene was inactivated [91]; by 4 months, adenomas and HCC [99]. +Recurrence of HCC in mice whose original tumors had regressed on Doxycycline | None reported | [91,99] |

(*continued on next page*)

**Table 2 (*continued*)**

| Gene | Type of mutation or tissue promoter/construct | Phenotype (+/− and −/−) | Chemically induced/ metastasis | References |
|---|---|---|---|---|
| Met and β-catenin | Transposable vectors containing wild-type human *MET*, constitutively-activated mutated form of β-catenin (*ΔN90-CTNNB1*), and dominant-negative TCF-1 (*DNHNF1*), by hydrodynamic transfection into livers | Combination *MET* and *ΔN90-CTNNB1*: 74% HCC within 1 month (no adenomas); combination *MET* and *DNHNF1*: 50% hepatic adenomas within 1 month; each one individually, no tumors | Death within 3 months | [99] |
| c-Met conditional knockout | c-Met conditional liver-specific knockout (MetLivKO) using floxed Met ($c\text{-}met^{fl/fl}$) and Cre driven by albumin promoter ($AlbCre^{-/-}$) | 100% HCC in MetLivKO at 6 months versus 44% in control; greater number and size of tumors in MetLivKO; protumorigenic effects of c-Met deficiency reversed by early administration of antioxidants | *N*-nitrosodiethylamine | [94] |
| TGFα | TGFα over-expression under metallothionein 1 promoter [86,87,90] | 10–15 mos: 50% HCC [87];100% HCC [86] +mammary/pancreatic hyperplasia [86,88] | Zinc in $H_2O$ increased tumor formation; no metastases | [86–88] |

The transgenic mouse expressing PreS, S and X proteins (Tg (HBV Alb-1) Bri44) described by Chisari et al. [52] has also been studied more extensively for its stepwise accumulation of liver disease. Gene expression in this model generates hepatocyte damage and inflammation early, generating dysplastic nodules by age 9 months, and macroscopic HCC nodules by age 18 months [53].

*3.2.2. Hepatitis C virus*

Hepatitis C virus (HCV) infects 170 million people worldwide, and the recent increase in HCC in the United States has been attributed to an increase predominantly among patients with chronic HCV infection. HCV does not cause insertional mutagenesis, but rather is thought to produce HCC through the cumulative effects of chronic infection, injury and repair. Most cases of HCC occur after several decades of infection with HCV and in a microenvironment of cirrhosis [54].

Several models have attempted to emulate HCV viral infection in hepatocytes in order to better understand its oncogenicity. Transgenic mice encoding the core, E1 and E2 structural proteins under control of the albumin promoter did not develop hepatic disease [55], although when the same strains were exposed to diethylnitrosamine (DEN), there were significantly larger HCC tumors in core-E1–E2 transgenic mice relative to the core and non-transgenic strains [56]. Koike et al. described two different mouse strains expressing HCV core protein under control of the HBV promoter; these mice developed steatosis after several months [57] and HCC in 32% of animals after 16–23 months [58,59]. The same study found no adenomas or carcinomas in transgenic mice over-expressing HCV envelope genes. Lerat et al. also described the development of HCC in mice transgenic for the entire HCV genome or core-E1–E2 structural genes under the control of albumin promoter [60].

The mechanism by which HCV core protein promotes oncogenesis is unclear. HCV core transgenic mice have been studied for their gene expression patterns, revealing that interleukin-1 (IL-1) and tumor necrosis factor (TNF) are transcriptionally activated in these models. Reactive oxygen species (ROS) are produced in HCV core transgenic mice even in the absence of hepatitis and inflammation [61]. Alcohol can act synergistically to produce ROS in HCV-core protein transgenic mice [62]. Clinically, heavy alcohol use is known to enhance the development of cirrhosis and HCC [60] in patients chronically infected with HCV; thus, production of ROS may be the common instigator.

*3.2.3. Woodchuck hepatitis virus*

Woodchucks develop cirrhosis and HCC from chronic Woodchuck Hepatitis Virus (WHV) infection. During the course of infection, WHV DNA is stably integrated into the DNA of 1–5% of hepatocytes [63], and causes HCC within the first 2–4 years of life [64]. Over 50% of these HCCs contain integrations of WHV DNA within, or immediately adjacent to, a unique and functional N-myc 2 retroposon, and are associated with increased IGF-2 expression [65].

*3.3. Experimental models recapitulating molecular events of hepatocarcinogenesis*

*3.3.1. Cell cycling pathways: p53, Rb, E2F, SV40 T antigen*

Cancer is a disease of the cell cycle in the majority of cases, as most tumors contain defects in cell cycle

machinery. Fundamental to our understanding of cancer biology have been models simulating loss of tumor suppressors p53 and Retinoblastoma (Rb), key regulators of cell cycling and frequent targets of carcinogens. There is a large body of evidence indicating a pivotal role for cell cycle deregulation during hepatocarcinogenesis [41].

Tumor suppressor p53 acts to restrict proliferation in response to DNA damage or deregulation of mitogenic oncogenes, by leading to the induction of various cell cycle checkpoints, to apoptosis, or to cellular senescence. p53 heterozygous mutant mice appear to be susceptible to HCC formation in the context of liver injury, but only in the absence of intact telomerase [66].

Trp53 knockout mice develop larger, more invasive tumors than wild-type mice when mouse polyoma virus middle T antigen (PyMT) viral oncogene is introduced into the liver under an albumin promoter [67]. Liver-specific knockout of Trp53 when combined with liver-specific PyMT expression also results in an invasive, metastatic phenotype. Concomitant loss of Ink4a/Arf tumor suppressor locus accelerates this process [68].

Lowe and colleagues assessed the extent to which p53 loss is required for maintaining established tumors [69]. To do so, they first transduced hepatoblasts *in vitro* with oncogenic *ras* (*HrasV12*) and a tet-responsive p53 shRNA (miR30 design short hairpin RNA), and then injected the cells into the spleen of nude mice. Next, they used RNA interference (RNAi) to conditionally regulate p53 expression in the nodules that had formed by transduced hepatoblasts seeding in the liver. The authors concluded that p53 loss can be required for the maintenance of aggressive carcinomas, and that the cellular senescence program can act together with the innate immune system to potently limit tumor growth.

The retinoblastoma (Rb) pathway plays its role in cell cycle regulation by guarding and triggering DNA replication and cell cycle division in late G1. Rb binds members of the E2F family, and in doing so represses transcription of E2F regulated genes, which mediate DNA synthesis and cell cycle regulation [70]. After noting upregulation of E2F in liver tumors from their c-myc/TGF-α double-transgenic mice, Conner et al. generated E2F transgenic mice under control of the albumin enhancer/promoter [71]. All of these mice formed adenomas after 10 months, and a minority developed HCC (2/6). When crossed with c-myc transgenic mice, HCC development was accelerated, with 100% tumor formation within 6–8 months. Further investigation of this model revealed activation of the Wnt/β-catenin pathway in a majority of the tumors, as demonstrated by accumulation of nuclear β-catenin; this occurred in the absence of mutations of β-catenin [72].

SV40 (Simian Vacuolating Virus 40) large T antigen (TAg) is an oncoprotein derived from the polyomavirus SV40 which is capable of transforming a variety of cell types. The transforming activity of TAg is due mainly to its perturbation of the retinoblastoma (pRB), p53 and p105 tumor suppressor proteins. This causes the cells to leave G1 phase and enter into S phase, which permits DNA replication of both the cell and the viral genome [73]. In addition, TAg binds to several other cellular factors, including the transcriptional co-activators p300 and CBP, which may contribute to its transforming capacity. SV40 T-antigen expression under the albumin enhancer/promoters provoked the appearance of adenomas and HCC within 3–7 months [74]. A tetracycline-inducible binary transgenic mouse model of SV40 was found to develop hepatic neoplasia in 60% of cases (3/5); no neoplasia was observed in mice with suppression of transgene expression by tetracycline administration [75].

### *3.3.2. Telomere dysfunction*

Telomeres are regions of DNA near the ends of eukaryotic chromosomes that act to prevent loss of genetic information during chromosomal replication. They are synthesized and maintained by telomerase, part of a group of enzymes called TERT (telomerase reverse transcriptases). Because of cell division mechanisms and because telomerase expression is repressed in most human cells (with the exception of stem cells and some leukocytes), telomere length decreases with each cell division. Once telomeres reach a critically short length, they unfold; this uncapping is detected and the cell undergoes senescence (the "Hayflick limit") [76]. Neutralization of p53 or Rb function results in continued telomere attrition, culminating in chromosomal instability and cell death [77]. Low levels of telomerase are associated with aging and tumorigenesis in some tumors such as colorectal cancer [78] but levels are typically increased in HCC [79,80].

Telomere attrition has been documented in hepatocytes from cirrhotic patients [81,82]. It is thought that repeated rounds of hepatocyte injury and regeneration may promote telomere shortening, which would ultimately lead to chromosomal instability (CIN), a common feature of HCC. Indeed a correlation between CIN, telomere shortening, and HCC was demonstrated in a series of 39 patients with HCC by analysis of liver biopsies for ploidy and telomere length [83].

In mice, reduction in telomere length is not observed, probably due to long initial telomere length and active telomerase expression [84]. However, in p53-mutant mice, deficiency of telomerase promotes formation of non-reciprocal translocations and epithelial cancers [85]. The cooperative roles of telomerase-induced chromosomal instability and attenuated p53 function in the liver was illustrated by a study which showed enhanced HCC formation in p53-mutated telomerase knockout mice ($mTERT^{-/-}$). In the setting of intact telomeres, however, p53 mutation had no effect on tumor formation [66].

*3.3.3. Growth factor signaling pathways*

*3.3.3.1. TGF-α and c-myc.* Transforming Growth Factor (TGF)-α binds and activates EGFR and is mitogenic toward hepatocytes. In most organs, metallonein-driven over-expression of TGF-α causes epithelial hyperplasia [41]. In liver and breast tissue, the phenotype extends to neoplastic transformation. Tumor incidence is 100% in susceptible mice strains after a substantial latency [86–88]. Gefitinib, an EGFR inhibitor, significantly reduces HCC development in rats with cirrhosis induced by DEN administration [89].

Co-expression of TGF-α and c-myc can occur in HCC. Liver-specific c-myc over-expression induces persistent hepatocyte proliferation and eventual HCC. When c-myc and TGF-α are co-expressed, this process is accelerated [90].

*3.3.3.2. Hepatocyte growth factor and c-Met pathway.* When stimulated by its ligand, hepatocyte growth factor (HGF) elicits multiple biological responses including proliferation, migration, invasion, and morphogenesis [91]. Over-expression, amplification, and mutation of the *MET* proto-oncogene which encodes protein tyrosine kinase receptor Met have been demonstrated in human HCC samples [92,93]. Nevertheless, experimental mouse models of HCC have revealed that the net outcome of HGF/c-Met activation could be either stimulation or inhibition of hepatocarcinogenesis [94]. Transgenic mice over-expressing HGF driven by the metallothionein promoter developed HCC [95], but when HGF expression was driven by the CMV promoter, mice developed hepatomegaly but not dysplasia [96]. Inhibition of hepatocarcinogenesis by HGF in c-myc transgenic mice was demonstrated by Thorgeirsson et al. in 1996: none of the liver-specific HGF/c-myc over-expressing mice developed HCC and only 30% developed adenomas, versus HCC in 60% of the c-myc single transgenic, even with addition of phenobarbital [97]. Similarly, HGF co-expression inhibited tumor formation in TGF-α transgenic mice [98].

The paradoxical effects of HGF ligand expression are mirrored in Met receptor expression. Bishop and colleagues demonstrated that over-expression of wild-type Met in hepatocytes of transgenic mice leads to the development of HCC [91]. Interestingly, these mice were found to have frequent activating mutations of β-catenin, and it was subsequently discovered that there was a correlation between MET activation and β-catenin mutations in human HCCs. Spurred by these findings, vectors of human MET and β-catenin with activating mutations were hydrodynamically cotransfected: these mice developed larger HCCs with short latency periods, confirming a cooperative relationship between *MET* over-expression and β-catenin mutations [99].

Recently, however, Takami et al. reported that loss of c-Met signaling enhanced rather than suppressed the early stages of chemical hepatocarcinogenesis [94]. C-met conditional knockout (MetLivKO) mice treated with *N*-nitrosodiethylamine developed significantly more and bigger tumors and with a shorter latency compared with control mice. These knockout mice had increased oxidative stress demonstrated signs of was reversed by administration of antioxidant *N*-acetyl-L-cysteine. The authors concluded that intact HGF/c-Met signaling is essential for maintaining normal redox homeostasis in the liver. Further studies will be needed before definitive conclusions can be drawn regarding the role of HGF/c-Met signaling in HCC.

*3.3.3.3. PTEN/Akt/mTOR signaling pathway.* The serine/threonine kinase Akt (PKB) was first isolated as an oncogene transduced by the acute transforming retrovirus [100,101]. Its role in human cancer was established shortly thereafter by demonstration of its frequent amplification and over-expression in various cancers, including breast and ovarian [102]. Akt acts as a cytoplasmic central regulator of numerous signals related to cell cycling (Cyclin D1), cell survival (Mdm2/p53), cardiovascular homeostasis (eNOS), and cell growth (mTOR), among others [103]. PTEN is a negative regulator of the pathway and its loss activates Akt.

Tissue-specific knockout models of PTEN in pancreas develop tumors with high penetrance [104]. Transgenic animals over-expressing Akt develop a hyperplasic but not malignant phenotype, typically requiring a second hit to generate cancer [105,106]. Notably, mTOR inhibition can reverse these phenotypes, suggesting the presence of an mTOR-dependent survival signal downstream of Akt [107]. Liver-specific deletion of PTEN results in hepatomegaly and steatohepatitis by 10 weeks and HCC in a majority of male mice by 20 months [108,109].

*3.3.3.4. IGF and EGF signaling pathway.* The insulin growth factor (IGF1 and IGF2) signaling pathways regulate cell growth, differentiation and survival, and play a central role in embryogenesis and regulation of lifespan. IGF-2 possesses both mitogenic and metabolic properties; 16–40% of human HCCs demonstrate over-expression of IGF-2 [110].

The coordinated expression of IGF-2 and its receptor suggests a role for IGF-2R in regulation of extracellular IGF-2 concentration; alterations in the expression of IGF-2R in human tumors suggest it may act as a tumor suppressor gene [111].

Transcriptional activation of IGF2 has been demonstrated in HCCs arising in HBV-associated human samples [112] and in HBV transgenic mice [41]. To investigate whether IGF-2 has a promoter role in a slowly developing HCC model, TGFα transgenic mice were crossed with IGF-2 hemizygous knockout mice

containing either only one maternal allele or two alleles. Imprinting usually blocks IGF-2 expression from the maternal allele in liver. However, IGF-2 re-expression occurred in all 4 of these models, and was chronologically associated with late stages of progression toward HCC [113].

Epidermal growth factor (EGF) is a potent mitogen to hepatocytes. Unlike in other malignancies, the EGF receptor is rarely mutated in HCC, and several reports suggest an EGF-mediated autocrine growth stimulation of hepatoma cells [114]. This was further supported by the accelerated liver tumor formation after constitutive over-expression of a secretable form of EGF (IgEGF). All double-transgenic mice with liver-specific IgEGF over-expression in cooperation with AAT-myc died by 4.4 months from HCC, whereas only 44% of ATT-myc mice had developed HCC by age 14 months [115].

*3.3.3.5. Wnt/β-catenin pathway.* A key pathway implicated in hepatic tumorigenesis is the canonical Wnt pathway, in which β-catenin acts as a co-activator of the TCF/LEF family of transcription factors and regulates the expression of several genes related to cell proliferation and apoptosis. The Wnt/β-catenin signaling pathway normally functions in cellular differentiation, proliferation, and apoptosis, and has a fundamental role in embryogenesis. Liver development in xenopus, zebrafish, and mouse embryogenesis has been shown to be dependent on functional Wnt signaling [116,117].

There is general agreement that Wnt signaling is upregulated in a subset of HCCs [118]. Mutations of genes encoding several components of the Wnt pathway have been described, including β-catenin (19–44%), AXIN1 and AXIN2 (5–14% and 3–10%) [119–123]. The mutations of β-catenin identified in HCC are located in exon 3 of the CTNNB1 gene, the phosphorylation site for GSK3α/β. In addition, immunohistological studies have demonstrated abnormal cytoplasmic and nuclear accumulation of β-catenin in 17–40% of human HCCs [124,125]. In addition to accumulated mutations, stimulation of proliferation in liver cancer cell lines transfected with Hepatitis C core viral protein is at least partially mediated by upregulation of Wnt-1 protein expression [126]. This correlation between HCV and the Wnt pathway needs to be verified by *in vivo* studies.

Although mutations in β-catenin are thought to be tumorigenic in human HCCs, transgenic mouse models over-expressing either a stable mutant form of β-catenin [127,128] or a constitutively activated, non-mutated form of β-catenin exhibit hepatomegaly, but no HCC [127–129]. Surprisingly, although mutations in the tumor suppressor APC are very rarely seen in HCC and patients with germline APC mutations do not typically develop HCC, it has been found that liver-targeted loss of APC in mice can lead to HCC through activation of β-catenin signaling [130].

It seems that a second hit from an additional mutation is required to generate tumors in β-catenin transgenic mice. Simultaneous co-expression of a Wnt-activating β-catenin mutation ($Catnb^{lox(ex3)}$) and mutation in H-ras introduced by adenovirus-mediated Cre expression resulted in HCC in 100% of the double-transgenic progeny [131]. The interplay between the growth factor signaling pathways and the Wnt/β-catenin pathway was amply illustrated in the simultaneous over-expression of HGF and β-catenin knockout mouse model generated by Monga and colleagues [96]: the proliferative effects of HGF over-expression were mediated by β-catenin stabilization, and were negated in β-catenin null mice.

*3.3.4. Other HCC models*

*3.3.4.1. Fibroblast growth factor in muscle.* While most mouse models of HCC express growth factors and oncogenes under liver-specific promoters, liver-specific expression is not a requirement for development of HCC. For example, a transgenic model over-expressing fibroblast growth factor 19 (FGF19) in skeletal muscle develops HCC in 53% of mice by age 10–12 months [132]. Interestingly, unlike the vast majority of both human tumors and murine models, these tumors are more common in female progeny. Hepatocellular proliferation was significantly increased in these mice and in non-transgenic mice injected with FGF19 protein. Furthermore, immunostaining for β-catenin revealed nuclear staining in 4/4 female mouse tumors, and subsequent sequencing of the GSK3β phosphorylation site of β-catenin revealed mutations in 16%, which implicates activation of the Wnt/β-catenin signaling pathway as a potential mechanism for hepatocellular transformation in this model.

*3.3.4.2. Urokinase-type plasminogen activator.* Not all genetically modified models of HCC arise from predicted oncogene over-expression, tumor suppressor loss, or liver injury. In a transgenic model over-expressing the urokinase-type plasminogen activator (*uPA*) transgene under the albumin promoter, for example, most mice died from liver hemorrhage within 4 days of birth; in the two transgenic lineages developed from surviving founder mice, there was a surprising 100% incidence of HCC at 8–20 months of age. Moreover, the surviving mice regained normal clotting function, and their livers were repopulated by clonal, regenerative nodules that no longer expressed the transgene. Tumor progenitor cells were found to contain transgene-deleting chromosomal rearrangements which likely extended into flanking DNA. Therefore, the initiating event in this HCC model was likely extensive DNA rearrangements occurring during rapid regeneration [133].

### 3.4. Chemically-induced fibrosis and hepatocarcinogenesis

Cirrhosis is a major cause of mortality as both a precursor to malignancy and a cause for liver failure. As a disease with clear environmental non-hereditary components to its aetiology, liver fibrosis and cancer is well suited for modeling using chemical induction. Experimental models of liver disease can be categorized as cholestatic, nutritional, alcoholic, immunological, and toxic, and have been reviewed elsewhere [134].

Briefly, several hepatotoxic agents have been used both in the induction of generalized liver disease and HCC (see Table 3). Chemical models of hepatocarcinogenesis often involve initiation by a carcinogen followed by a growth stimulus promoter to induce clonal expansion of initiated cells, such as partial hepatectomy (Solt–Farber method [135]) or phenobarbital [136]. Alternatively, rodents are subjected to repeated administration of carcinogens such as DEN, DMN, or $CCl_4$ over a prolonged period [136]. Most initiated cells accrue damage and ultimately undergo apoptosis, but the small number that respond to promoters evolve into dysplastic foci and later to dysplastic nodules. These foci and nodules can disappear following the removal of promoters in a process termed remodeling, which typically involves apoptosis of the preneoplastic cells [41]. Nodules which have acquired the capacity for autonomous growth progress to neoplastic nodules and HCC, an irreversible process involving the accumulation of genomic damage [137].

The most commonly employed model for liver disease is carbon tetrachloride ($CCl_4$) administered in drinking water, in inhaled gases, or by intraperitoneal injection. The reactive metabolite trichloromethyl radical is produced during the oxidative metabolism of $CCl_4$ by cytochrome p450, and causes liver damage by eliciting production of reactive oxygen intermediates and by peroxidative degradation of membrane phospholipids [138]. Compounds like phenobarbital, ethanol, and acetone induce microsomal cytochrome p450 and therefore potentiate the hepatotoxicity of $CCl_4$, as does hypoxia; therefore, hepatocellular injury and necrosis are predominantly seen in the centrolobular zone where the oxygen tension is low [134,138].

Dimethylnitrosamine (DMN) is a carcinogenic agent which causes liver injury by covalent binding and methylation of nucleic acids and proteins in hepatocytes [139]. Animals administered DMN either per oral or by intraperitoneal injection develop cirrhosis within 3–4 weeks, and can continue to have stable or progressive disease for several months after discontinuation of the agent [140].

Diethylnitrosamine (DEN) induces pericentral foci of small dysplastic hepatocytes and acts by ethylating nucleophilic sites in DNA [141,142], causing cirrhosis and multifocal HCC within 18 weeks [89,143]. Frequent β-catenin mutations have been found in HCCs induced by DENA in mice [144], and when combined with a methyl-deficient diet, DEN administration generates p53 mutation or rearrangement in rats [145].

Thioacetamide (TAA) in drinking water (0.03%) or by intraperitoneal injection induces fibrosis in rats and mice over a period of 2–3 months, which may be secondary to the oxidant properties of TAA and the induction of hepatic oxidative stress [134,146,147]. Acute liver injury and subsequent fibrosis can be created by administration of D-galactosamine (GalN), a hepatotoxin that induces liver damage by depleting uridine nucleotides and therefore diminishing RNA and protein synthesis [148].

Cholestatic cirrhosis has been induced by extrahepatic bile duct ligation (BDL) in rats, rabbits, dogs, and monkeys. Histologically, the BDL model is characterized by infiltration of connective tissue in the portal

**Table 3**
**Toxic models of liver fibrosis and HCC**

| Diet or chemical | Mechanism of action | Phenotype | References |
|---|---|---|---|
| Choline-deficient and ethionine (CDE) diet | Oxidative DNA damage, DNA strand breaks and chromosomal instability [41] | 30–35 weeks: 100% HCC | [135,190–192] |
| Ciprofibrate | Synthetic peroxisome proliferators, non-genotoxic carcinogen | 60 weeks: 100% HCC [193] | [90,193,194] |
| Diethylnitrosamine (DENA) | Genotoxic hepatocarcinogen | 100% HCC in males, 30% in females. Extensive chromosomal damage | [90,168,194,195] |
| Thioacetamide (TAA) | Metabolites induce oxidative stress | 100% HCC | [134,146] |
| 2-Acetylaminoflouren (2-AAF) | Genotoxic | Used primarily as promoter in initiation/promotion protocols | [194,196] |
| Phenobarbital | Non-genotoxic | Used as promoter in initiation/promotion protocols; increases HCC by 500%. Can inhibit tumor formation in mice given DEN. Associated with β-catenin activation [197] | [197,198] |